Metal-Based X-ray Contrast Media

Shi-Bao Yu and Alan D. Watson*

Torsten Almén Research Center, Nycomed Amersham Imaging, 466 Devon Park Drive, Wayne, Pennsylvania 19087

Received March 1, 1999 (Revised Manuscript Received June 16, 1999)

Contents

Shi-Bao Yu was born in Henan, PR China, in 1960 and graduated from Fudan University in Shanghai (B.S.) and Harvard University (Ph.D. with Professor R. H. Holm). After a post-doctoral fellowship at MIT (with Professor S. J. Lippard), he joined Nycomed Salutar as a scientist working on the research and development of new contrast agents for X-ray and magnetic resonance imaging. Currently, he is a principal research investigator with Nycomed Amersham, and his research interests include targeted diagnostic and therapeutic agents.

Alan D. Watson was born in Canberra, Australia, in 1952. He earned his B.Sc. (Hons) degree at the University of New South Wales and his Ph.D. degree in bioinorganic chemistry from the Australian National University (with Alan Sargeson) in 1979. Following post-doctoral appointments at Leeds University (with A. Geoffrey Sykes) and Harvard University (with Richard H. Holm), he joined DuPont Pharmaceuticals in 1983 to develop technetium-based complexes as radiopharmaceuticals. This work culminated in the discovery of Neurolite, a technetium-based brain imaging product launched by DuPont in 1992. He moved to Salutar Inc. in Sunnyvale, CA, in 1988 to work on metal-based magnetic resonance imaging (MRI) contrast agents and continues to work broadly in all aspects of contrast media research and development for Nycomed Amersham in Wayne, PA. His scientific interests currently focus on the research and development of novel gas-containing microbubble emulsions for use as ultrasound contrast agents as well as metal chelate-based drugs for use in the MRI, X-ray, and radiopharmaceutical fields.

I. Introduction

The discovery of X-ray radiation by Wilhelm C. Roentgen in 1895 revolutionized the practice of medicine.[1,2] Physicians instantly recognized the importance of X-ray radiation in medical diagnoses since one could now externally visualize the internal anatomic structures of a patient without surgery. Today, diagnostic imaging procedures are a routine part of modern medicine, useful in performing the initial diagnosis, the planning of treatment and post-treatment evaluation.

10.1021/cr980441p CCC: $35.00
Published on Web 08/12/1999

By one estimate, 300 million diagnostic examinations are performed annually in the United States.[3] Even with the recent phenomenal growth of MRI and ultrasound procedures, X-ray imaging studies remain the workhorse of modern radiology (currently 75−80% of all diagnostic imaging procedures are X-ray related).[4−6] The famous first unenhanced X-ray image (Figure 1) of Mrs. Roentgen's hand demonstrates

Figure 1. The first X-ray image: Mrs. Roentgen's hand.

superb visualization of bone structures due to the inherent contrast between electron-dense bones and the surrounding more permeable soft tissues. However, the native contrast between the different soft tissues that make up the human body is so small that unenhanced X-ray imaging cannot differentiate between them.

To better delineate soft tissue regions such as the cardiovascular system, safe and efficient X-ray contrast agents (also called radiographic contrast agents, radiopaque agents, or roentgenographic agents) were long sought after. Contrast agents are a class of pharmaceuticals that, when administrated to a patient, enter and pass through anatomic regions of interest to provide transient contrast enhancement. Preferably, these agents are then essentially completely excreted from the patient without being metabolized. There are two types of X-ray contrast agents currently approved for human use: barium sulfate suspensions, which are used strictly for gastrointestinal (GI) tract imaging, and water-soluble aromatic iodinated contrast agents. The earliest use of a barium contrast agent for GI imaging can be traced back to 1910.[7] Now, inexpensive $BaSO_4$ formulations are routinely used in about 5 million X-ray procedures per year in the United States.[5,6] Over the last 90 years, there have been incremental improvements in these formulations which have improved their tolerability and tissue coating characteristics.[8,9] However, there is little research activity in this area at the present time primarily due to the lack of adequate commercial incentives.

By comparison, iodinated agents have experienced a much more significant evolution with a series of new molecular entities replacing a range of older materials and then being pushed aside in turn by improved newer-generation products.[10−12] The long and rich history of iodinated agents began in 1923 when Osborne and colleagues at the Mayo Clinic noticed that either oral or intravenous administered sodium iodide solutions opacified the bladder.[13] In the late 1920s Swick, in collaboration with the chemist Binz, developed Uroselectan (sodium 5-iodo-2-pyridone-*N*-acetate) as an intravenous contrast agent for urography (urinary tract imaging).[14,15]

Modern water-soluble iodinated agents utilize the 1,3,5-triiodobenzene platform which first appeared, as diatrizoic acid or diatrizoate, in 1954.[10] Since that time, four separate classes of active molecules based on this aromatic platform have emerged. Representatives of each class are depicted in Figure 2, and selected physical properties are listed in Table 1.[16]

Ionic triiodobenzene monomers (such as diatrizoate) were the first generation of X-ray contrast agents developed for general intravascular use. The low toxicity and high water solubility of these agents, compared with previous materials, resulted in their completely replacing older iodinated agents. However, these agents are not completely benign; moderate and even severe (although with a very low incidence) cardiovascular, anaphylactic (allergic) and pain reactions may occur with their use.[17] The extent of the pain reactions were particularly limiting in certain applications such as intrathecal injections (directly into the cerebrospinal fluid) for myelography (spinal cord imaging).

The next major advance in the development of X-ray contrast agents occurred in the late 1960s based on a seminal contribution by Torsten Almén, a clinical radiologist at the University of Lund, Sweden.[18,19] Almén hypothesized that the observed chemotoxicity of the common ionic agents was not the most significant contribution to the adverse event profile noted in clinical use; more likely, this chemotoxicity was due to overloading the homeostasis of the body by the rapid addition of large quantities of high-osmolality material. Novel second-generation, nonionic, water-soluble iodinated contrast media were quickly developed during the 1970s which had significantly lower osmolality. The extent of severe adverse reactions and the degree of pain upon injection were greatly reduced following the widespread adoption of these agents, and they have now largely replaced first-generation agents. A new class of contrast media with significantly lower osmolality than the nonionic monomers is now emerging. In fact, nonionic dimers, formulated to be isotonic to blood, have demonstrated even

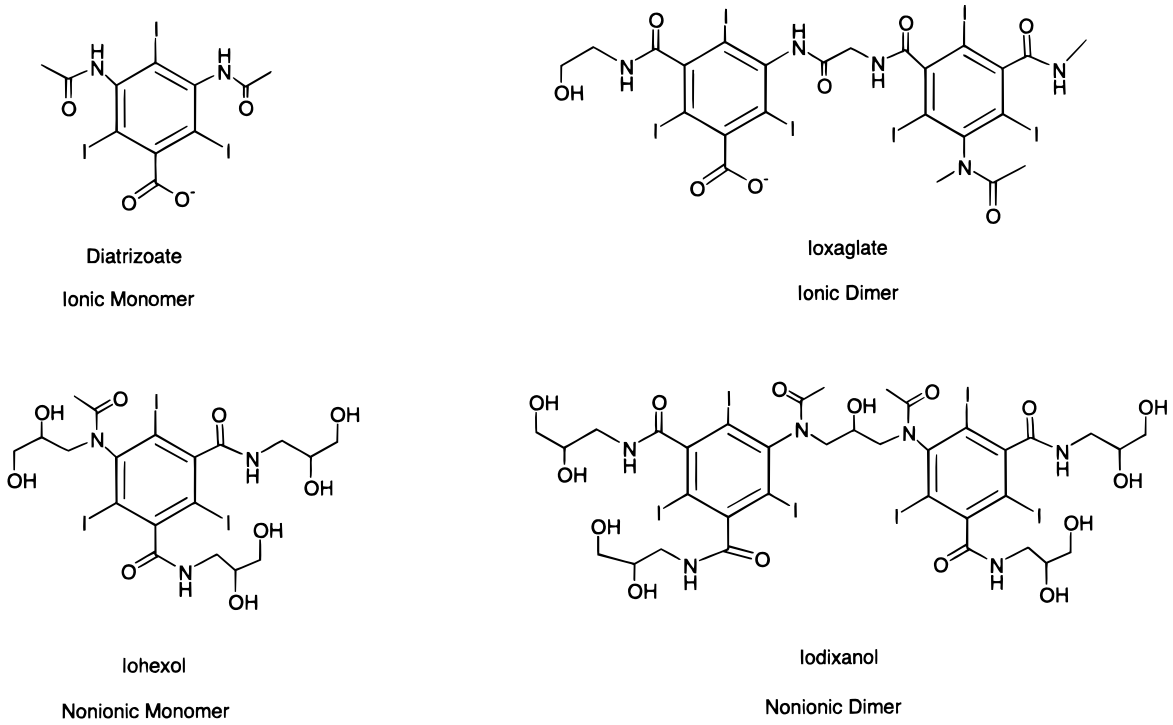

Figure 2. Chemical structures of representative of iodinated X-ray contrast agents.

Table 1. Physical Properties of Selected X-ray Contrast Media

	diatrizoate	ioxaglate	iohexol	iodixanol
class	ionic monomer	ionic dimer	nonionic monomer	nonionic dimer
iodine atoms per particles in solution	1.5	3	3	6
particle molecular weight	613	1268	821	1550
I%	62.1	60.1	46.4	49.1
partition coefficient[a]	0.044	0.086	0.082	0.028
osmolality (osm/kg; for 300 mg of I/mL solution)	1.57	0.56	0.67	0.29[d]
viscosity (cp; 37 °C for 300 mg of I/mL)[b]	4.2	6.2	6.3	11.8[d]
density (g/mL; 20° C for 300 mg of I/mL)	1.34	1.32	1.35	1.37[d]
LD_{50} {mmol/kg, (g of I/kg in parentheses)}[c]	20 (7.5)	17.6 (13.4)	63.5 (24.2)	27.6 (21)

[a] Butanol/water. [b] Viscosity for water is 1 cp. [c] The dose producing acute death in 50% of the animals (mice) after the administration (one min intravenous injection) of a drug substance (contrast media). [d] Data for iodixanol is for 320 mg of I/mL solution.

greater patient acceptance in certain radiological applications.[20]

Today, iodinated X-ray contrast agents are used in about 20 million procedures annually in the United States, mainly in computed tomography (CT, vide infra) and angiographic applications. Sales of these agents in the United States exceeded $550 million in 1997.[5,6]

This review focuses on research efforts to develop a completely different category of X-ray contrast agents, based not on barium or iodine but on electron-dense heavy metals. A brief primer on the medical physics of X-ray contrast media is followed by a survey of historical and contemporary investigations into the use of metals and heavy metal compounds as X-ray contrast agents. Together with physicochemical and structural characteristics, major clinical and preclinical investigations (including pharmacological and toxicological studies) are described. Finally, we will take a brief look at current research efforts and possible future prospects for additional breakthroughs in this field.

II. Medical Physics of X-ray Contrast[21]

A. X-ray Generation

X-rays are generated by energy conversion when accelerated electrons from the cathode of the X-ray tube interact with atoms of an anode target. There are two processes for this energy conversion: bremsstrahlung and characteristic radiation. When fast moving electrons hit the target, they are rapidly decelerated due to multiple collisions with target nuclei. The kinetic energy lost by the electrons is emitted directly in the form of X-ray photons. Since these electrons do not have the same initial energy and most electrons lose their energies in stages, a radiation continuum of X-rays (general radiation or bremsstrahlung) is generated by this process. When electrons of certain critical energies collide with electrons in the innermost shell (K shell) of the atoms of the anode target, they can eject these electrons out of their atomic orbits. This vacancy is filled by descending electrons from the next higher shell (M) or the one above it (L), again with an emission of

radiation. This process produces X-rays that are characteristic of the target atoms (M → K: $K_{\alpha 1}$, $K_{\alpha 2}$; L → K: $K_{\beta 1}$, $K_{\beta 2}$).

The voltage applied to an X-ray tube is expressed as its peak kilovoltage (kVp), while the energy of the resultant X-ray photons generated is expressed in kiloelectronvolts (keV). In medical imaging, tungsten is usually selected as the X-ray tube target material. Its high atomic number ($Z = 74$) makes it more efficient for the production of X-rays than lower Z materials. A plot of X-ray intensity vs photon energy from a tungsten X-ray tube is shown in Figure 3. The

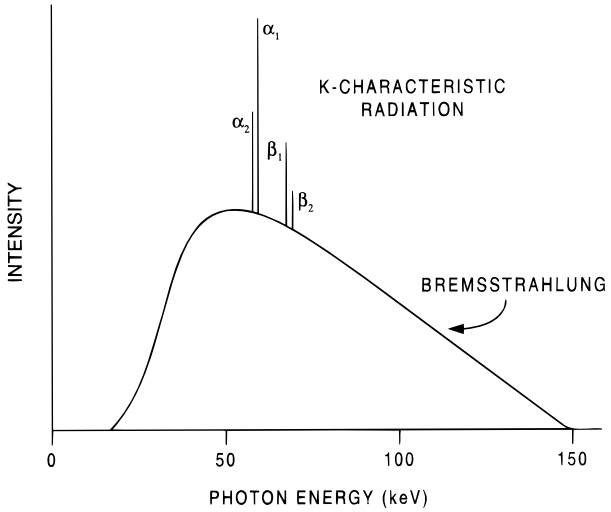

Figure 3. Typical X-ray emission spectrum from a tungsten X-ray tube operating at 150 kVp with aluminum filtering.

tube voltage is set at 150 kVp. This X-ray emission spectrum is a combination of general radiation and characteristic radiation. The maximum photon energy is 150 keV, and the low-energy X-ray photons are removed by the X-ray tube enclosure and internal aluminum or copper filtration. The X-ray energy spectrum has a maximum intensity around 45−50 keV, and the characteristic radiation emitted is between 57 and 69 keV. The contribution of characteristic radiation to total X-ray production is between 10% and 30% when the tungsten X-ray tube is operated at 80−150 kVp. For procedures such as breast imaging that require low-energy X-ray radiation, a molybdenum target (which yields X-ray radiation mostly in the lower energy region and then primarily from the contribution of its characteristic radiation) is used.

An increase in tube voltage (kVp) will shift the X-ray photon energy spectrum to the right, i.e., more photons are produced in the high-energy region. An increase in electric current (mA) however, only increases the intensity of the X-ray radiation with no shift in the distribution of photon energy.

B. X-ray Attenuation

When an X-ray beam traverses matter both absorption and deflection of photons will occur. The reduction in beam intensity due to these processes defines the degree of X-ray attenuation and it obeys the following equation

$$I = I_0 e^{-\mu x} \quad (1)$$

where I is the transmitted X-ray intensity, I_0 is the incident intensity, and x is the thickness of the matter (absorber). The mass attenuation coefficient of the absorber, μ, is expressed in cm^2/g.

Figure 4 is a schematic representation of a patient

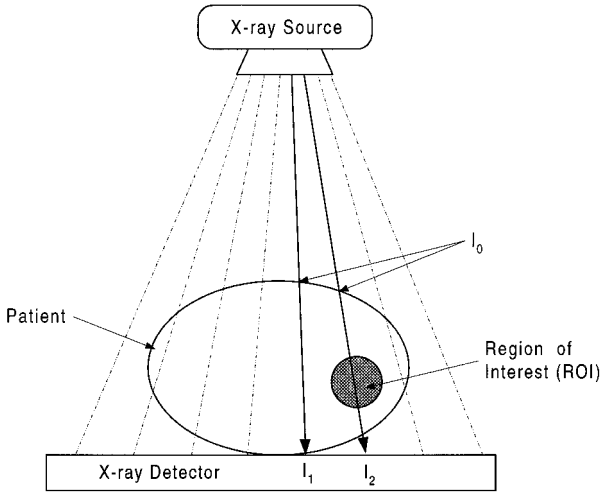

Figure 4. Schematic drawing of a patient undergoing an X-ray diagnostic imaging procedure.

with a particular clinical region of interest (ROI) undergoing an X-ray diagnostic imaging procedure in its simplest form. The incident X-rays have intensity I_0, and after passing through the body, two transmitted X-rays are detected with intensity I_1 and I_2. The percentage difference between I_1 and I_2, $(I_1 - I_2)/I_1$ is defined as the degree of X-ray contrast and is a function of the mass attenuation coefficients and the thicknesses of the different tissues.

$$(I_1 - I_2)/I_1 = 1 - e^{-(\mu_2\chi_2 - \mu_1\chi_1)} \quad (2)$$

The greater the contrast, the better the ability to identify an ROI against a background of normal surrounding tissues. Thus, a primary goal for a radiologist in any diagnostic imaging procedure is to obtain the greatest contrast differential possible between healthy and diseased tissues.

X-ray attenuation comes from three interactions between X-ray photons and traversed matter in the energy range meaningful for diagnostic imaging: coherent scattering (ω), the photoelectron effect (τ), and Compton scattering (δ). The mass attenuation coefficient (μ) is the sum of these three interactions:

$$\mu = \omega + \tau + \delta \quad (3)$$

Coherent scattering produces scattered radiation and contributes to noise on X-ray films, but it is so minor as to be excluded from further consideration. The photoelectron effect comes from the interaction of the X-ray photons with inner-shell electrons. When an incident photon impacts an electron with energy greater than the binding energy of the encountered electron, it can eject the electron from its orbit. Since all its energy is given up in this process, the incident photon is absorbed and disappears. The ejected

electron (a so-called free electron) is absorbed immediately. The vacancy left in the inner shell is immediately filled by an electron from an outer shell, producing another characteristic radiation emission. This radiation, however, will have a lower energy and its direction will be random. The photoelectron effect is most likely to result when the X-ray photon energy is greater yet almost the same as the electronic binding energy. Therefore, the greater the photon energy, the less X-ray absorption will occur in this process. In fact, τ is inversely proportional to the third power of photon energy E:

$$\tau \propto 1/E^3 \quad (4)$$

On the other hand, when the K shell electrons have high binding energies, such as those absorbers with high Z, they are more likely to be involved in the photoelectron effect and τ is proportional to the third power of Z:

$$\tau \propto Z^3 \quad (5)$$

In summary, the contribution of photoelectron effect to X-ray attenuation is high with low-energy X-ray radiation and with absorbers of high Z. It produces almost no scattering radiation and results in a high-quality image. However, since most of its energy is being absorbed, it exposes the patient to a high dose of radiation.

Compton scattering (δ) arises from the interaction of an X-ray photon with an outer-shell electron. When an X-ray photon with high energy collides with an outer-shell electron (its binding energy is relatively small), it will eject the electron from its orbit. The photon itself will be deflected as scattered radiation in a new direction with a lower energy. The probability for Compton scattering depends on the total number of electrons in an absorber and is independent of the atomic number. In fact, while Compton scattering dominates X-ray attenuation for matter with low Z at high energy, its contribution is greatly diminished for matter with high Z as the photoelectron effect predominates. Compton scattering is responsible for almost all scattered radiation, which both increases noise and decreases contrast. The quantity of Compton scattering gradually diminishes as the X-ray photon energy increases, so that high-energy photons are more likely to pass through the body than low-energy photons. As a result, the radiation exposure to patients is lower with high-energy X-rays than that with low-energy X-rays.

C. Contrast Enhancement

From the standpoint of minimizing radiation exposure to patients, it would be preferable to carry out all X-ray procedures using high-energy X-rays. However, as indicated earlier, X-ray attenuation is also a function of photon energy. Figure 5 plots the mass attenuation coefficients of bone, muscle, and fat together with selected heavy elements against X-ray photon energy. The differences between mass attenuation coefficients of body tissues, which produce the inherent contrast between them, become smaller, decreasing to almost background levels as X-ray photon energy increases. Since very low energy X-rays will produce unacceptable radiation doses to patients and high-energy X-rays diminish the inherent contrast, X-ray energies used in current medical imaging procedures represent a compromise between optimal image quality and patient radiation dose. The inherent contrast between bone and other tissues is large enough for clinical use in the low to middle X-ray energy range. However, using a tungsten X-ray tube with filtering, the inherent contrast between fat and muscle (two representative soft tissues) is too small to be clinically useful. To better delineate such tissues, contrast enhancing agents with differential uptake in different tissues of the body are required.

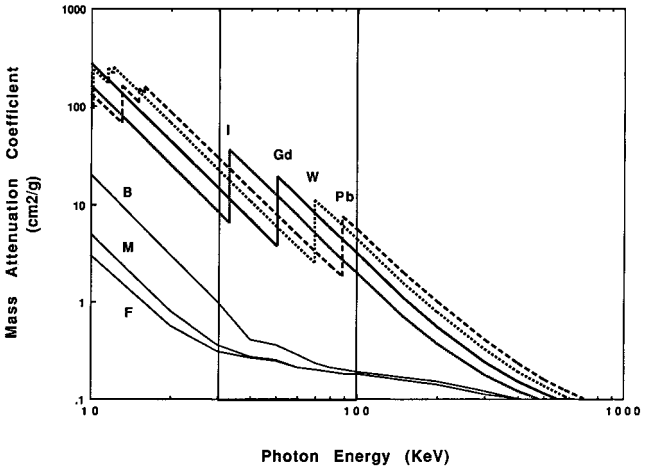

Figure 5. Mass attenuation coefficients vs photon energy.

All contrast agents contain a heavy element that effectively contributes almost all the X-ray contrast attenuation produced by such materials. Contrast enhancement comes largely from the photoelectron effect due to high atomic numbers, e.g., for iodine Z is 53 and for barium Z is 56. The photoelectron effect also explains the sharp increase in mass attenuation coefficients at the K-shell electron binding energy (K edge). Table 2 lists atomic numbers and K edge energies for iodine, barium, and other selected heavy elements. When one considers the X-ray photon energy spectrum generated by a tungsten tube (Figure 3), the mass X-ray attenuation coefficient diagram in Figure 5, and the K edge of the heavy elements, it can be concluded that current clinical

Table 2. K-Shell Electron Binding Energies (K Edge) for Selected Heavy Elements

element	atomic number	K edge energy[a]
I	53	33.2
Ba	56	37.4
Ce	58	40.4
Gd	64	50.2
Tb	65	52.0
Dy	66	53.8
Yb	70	61.3
W	74	69.5
Re	75	71.7
Au	79	80.7
Pb	82	88.0
Bi	83	90.5

[a] *CRC Handbook of Chemistry and Physics*, 66th ed.; Weast, E. C., Ed.; CRC Press: Boca Raton, FL, 1986, F-170.

use of iodine as a general X-ray contrast agent is not optimal, since its attenuation characteristics are mismatched with the X-ray photon energy of a tungsten tube. Other heavy elements can be better matched with X-ray photon energies for X-ray attenuation. It is possible to fine-tune X-ray attenuation by selecting a heavy element whose attenuation characteristics match the X-ray photon energy that is being used. The current use of iodinated X-ray contrast agents is, therefore, largely based on their superior safety and cost rather than their optimal efficiency as X-ray attenuators.

Several theoretical and experimental investigations have demonstrated the superior X-ray contrast enhancing ability of heavy metal elements.[22−25] A CT phantom study revealed that under normal operating conditions (120 kVp), heavy elements with Z between 58 and 66 produced higher X-ray contrast than iodine.[26] A new X-ray contrast agent based on heavy elements would have two advantages: a higher intrinsic contrast and a lower radiation exposure to patients.

The degree of X-ray contrast produced by the current generation of iodinated agents has proven to be inadequate for some procedures: a higher degree of intrinsic X-ray contrast afforded by heavy elements could potentially better address clinical needs in those procedures. In addition, from an efficiency standpoint, heavy element-based contrast agents would be competitive with iodinated agents in most regular radiological applications. The amount of material that would be needed to produce equivalent contrast could be decreased, and so the total volume could be lowered if the material is highly water-soluble; a lower dosage of an X-ray contrast agent is always desirable. Finally, as these agents have higher K edges and, therefore, greater X-ray attenuations at higher X-ray photon energies, the overall radiation exposure to patients would be reduced.

D. X-ray Diagnostic Medical Procedures[27]

After an X-ray beam passes through a patient, the spatial variation of the X-ray intensity of the emergent beam contains the medical information that is obtained from the procedure. Since human eyes cannot see an X-ray beam, one needs to transfer this information to a suitable medium for viewing and for long-term storage. This information transformation acts as a "decoding" process and unfortunately always results in the loss of some information (resolution). Attempts to reduce this loss of information have resulted in new radiological procedures, particularly employing modern computing technology.

Four major groups of X-ray diagnostic procedures are in practice today, classified by the techniques to transform and record X-ray contrast information: photographic film, X-ray fluoroscopy, computed tomography (CT), and digital subtraction angiography (DSA).

The direct action of X-rays can expose a film. More commonly, the energy of X-ray photons is converted into light by intensifying screens and this light is used to expose film. The film is then developed, and an X-ray image (radiograph or radiogram) is obtained. The degree of film blackening is directly related to the intensity of the radiation reaching the film or intensifying screen—the more X-rays absorbed by a region, the whiter that region appears on film. Plain film imaging is the most commonly used radiographic procedure, typically using the inherent natural contrast differences between air, fat, and bone. Bones appear white on an X-ray film since they absorb more X-rays (positive contrast), while air and fat appear black or gray as they allow more X-rays to pass through them (negative contrast).

The measurement of film "blackness" is called the photographic density (D)

$$D = \log(I_0/I_t) \tag{6}$$

where I_0 is the light intensity incident on a film and I_t is the light intensity transmitted by the film—the ratio of I_0/I_t is called opacity. Radiologists generally talk in terms of radiodensity and radiopacity, which are actually the opposite of photographic density and opacity. A contrast agent is said to have a high radiodensity if it absorbs more X-ray photons and produces positive contrast on X-ray film (whitening, such as with bone), i.e. its photographic density or opacity is low.

Roentgen's discovery of X-radiation was based on its ability to cause fluorescence in fluorescent materials. The fluoroscopic image generated by an X-ray beam after it passes through a human body contains similar diagnostic information to that captured on X-ray film. Advances in image intensifier design and CCD camera technology have allowed a fluoroscopic image of a human body to be easily visualized. Historically, the fluoroscopic image from an image intensifier screen was captured on spot films. Electronic storage systems such as magnetic tapes and video disks are now commonly used to record and store X-ray fluoroscopic images.

Digital subtraction angiography (DSA) is a generic term for any digital radiographic method of implementing subtraction angiography. Digital fluoroscopy, for example, is one common type of digital radiography system in which a digital image processing unit is used to convert an analogue image from the conventional fluoroscopic unit to a digitized image. The digital data is then stored in and manipulated by a computer. The most common DSA technique is mask subtraction—a digital image recorded precontrast (mask image) is subtracted from the digital image recorded after the injection of the contrast material. DSA is particularly useful in performing angiographic studies where the background to the vascular tree is irregular and dense, for example, in the base of the skull and in the upper chest. By canceling out the background only the vascular structures remain visible.

Computed tomography (CT) describes a general radiographic technique used to produce cross-sectional (tomographic) images of the human body. First, a cross-section of the body is scanned with a narrow X-ray beam from multiple angles. Then the linear attenuation coefficients for each tiny block (a voxel) in the cross-section are calculated. Finally, the to-

Table 3. X-ray Diagnostic Procedures by Body System

body system	diagnostic procedures	technique	share[a]
vasculature	angiography, arteriography (arteries), venography (veins), ventriculography (chambers of the heart) and interventional angiography	*iv* or *ia* administration of soluble contrast media during image acquisition. Patient is catheterized to permit administration of the agent near the region of interest. Interventional procedures include vessel remodeling procedures such as angioplasty, stent placement and atherectomy, all of which are conducted using angiographic visualization. Angiographic procedures tend to use large quantities of highly concentrated contrast media.	17%
organs	brain CT, abdominal CT, liver CT, hepatosplenography (liver and spleen X-ray), iv pyelography (kidney) and cholecystography (gallbladder)	Generally includes *iv* administration of contrast agent prior to image acquisition. Agents frequently administered as infusions. Delay permits agent to accumulate is specific tissues such as tumors. Often before and after contrast images are acquired.	54%
spinal canal	myelography (spine) and cisternography (brain)	Direct injection of contrast agent into the spinal canal or subarachnoid space. May be a very painful procedure and uses small volumes of low-concentration nonionic agents.	2%
urinary tract and bladder	retrograde pyelography and urethrography	Contrast administration through catheter placed in bladder.	3%
gastrointestinal	upper and lower GI	Administration of insoluble agents into upper (orally or via catheter) or lower (enema) GI tract. Air may be administered to inflate organs.	22%
joints	arthrography and diskography	Injection of contrast agent directly into the joint.	1%
uterine cavity and fallopian tubes	hysterosalpingography	Contrast media introduced to uterus and/or into fallopian tubes.	1%

[a] Percentage of all U.S. contrast-enhanced X-ray based procedures (includes X-ray, CT and fluoroscopy) in 1998.

mographic image is reconstructed with a computer and displayed on a monitor as a gray scale image. Unlike other X-ray techniques, CT is extremely sensitive to slight differences in tissue densities and is capable of differentiating a variety of soft tissues without the aid of contrast agents. However, contrast agents play an important role in many CT examinations. With the administration of a contrast agent, additional information critical to the diagnosis can often be obtained.

In CT, the linear X-ray attenuation coefficient of a voxel is directly measured, and so a CT number is defined as

$$\text{CT number} = K(\mu_p - \mu_w)/\mu_w \qquad (7)$$

where K is a magnification constant, μ_p is the linear attenuation coefficient of a pixel (which is the image element corresponding to a voxel) in the region of interest, and μ_w is the linear attenuation coefficient of water. When K is 1000, then the CT numbers are called Hounsfield units (HU).

Table 3 lists a number of the more common X-ray diagnostic procedures which presently utilize contrast media, organized according to body system and route of administration. The relative frequency of the procedures are also indicated and show that the general intravascular administration procedures, which include organ imagery and angiography, are the most significant in terms of soluble contrast agent utilization.[28]

III. Metals, Metal Salts, and Metal Particulates as X-ray Contrast Agents

Following the discovery of the ability of X-ray radiation to generate images, Roentgen went on to demonstrate that various materials, whether they are gases, liquids, or solids, are as transparent to X-radiation as is air. However, he noted that sheets of copper, silver, lead, gold, and platinum showed varying degrees of transparency. He concluded that the X-ray transparency of a substance primarily depends on its density. He also found a related phenomenon regarding glasses. Although generally transparent to visible light, glass showed varying degrees of X-ray transparency, which was inversely proportional to the amount of lead incorporated into the material.[1,2] These findings immediately became the basis for the search for X-ray attenuating contrast agents, although such endeavors were severely hampered by the limited availability of heavy metals at the time. When the usefulness of one X-ray contrast agent was demonstrated in one particular radiological application, it was a common practice for physicians to explore additional uses, often with little understanding of the underlying pharmacological and toxicological properties of such materials. The focus of early contrast agent research was purely on efficacy. The goal for physicians was to gain diagnostic insights and safety concerns regarding such materials were often completely overlooked.

A. Silver

As early as 1905, Collargol (a colloidal silver preparation) was used in urinary tract radiography.[29] Later, various silver preparations, including salts such as AgI and Ag_2O, were used as contrast materials in retrograde pyelography.[30] This procedure was not only quite useful in the diagnosis of dialation, kinking, and displacement of the renal pelvis and ureter, but also in the detection of renal malformations and renal tumors.

However, use of these silver agents was quickly discontinued since their administration could cause severe side effects and even death.[2] In addition, new, less toxic, iodinated contrast materials were by then becoming available.

Even as recently as 1979, silver iodide colloid was used as a model compound in an animal study to determine the suitability of metal particulates as hepatobiliary contrast agents for CT.[31] Silver colloid remained in the liver long enough to allow a CT examination, and the opacification of the liver increased 4- to 5-fold over background. However, toxicity precluded any use of this agent in human subjects.

B. Bismuth

Bismuth salts (bismuth subnitrate in particular) were perhaps the earliest X-ray contrast agents for general use in human patients. Radiologists had easy access to these materials as they were, and continue to be, widely used as remedies for GI ailments. For this reason, radiologists often had "accidental" encounters with bismuth compounds, which provided numerous opportunities to utilize the X-ray contrast enhancing ability of bismuth. The first radiograph of a bismuth-enhanced segment of the GI tract was made in 1897 using a 5% suspension of bismuth subnitrate.[32] A year later bismuth meals or syrups were developed for X-ray examinations of the whole GI tract.[33]

The first contrast-enhanced coronary angiogram ever obtained was from a human cadaver using a bismuth subnitrate emulsion.[34] Bismuth compounds were also investigated for use in bronchography (insufflation of bismuth subcarbonate powder to map out the tracheo-bronchial tree)[35] and retrograde pyelography (a mixture of bismuth subnitrate was able to demonstrate a bladder abnormality).[36]

The use of bismuth compounds for GI imaging did not continue. High doses of bismuth subnitrate are poisonous. In addition, bismuth salts were quite expensive. Eventually they were replaced by cheaper, nontoxic, and easy to make barium sulfate preparations which produced GI images of equal contrast enhancement to those obtained with bismuth.

Currently, bismuth subcarbonate is being considered as an X-ray contrast enhancing additive for dental filling composites[37] and bismuth oxide is being evaluated as a coating material for intravascular catheters to improve their visibility under X-ray fluoroscopy.[38]

C. Cesium

Cesium salts, in particular, CsCl and cesium bitartrate, were investigated as contrast agents for bronchography and for uterine and fallopian tube imaging.[39] In a bronchography application, cesium solutions (e.g. CsCl, 10−20 mL, 30%) were injected into the trachea of dogs. No obvious toxic reactions were observed and radiopacity was good. However, the cesium salts were completely absorbed from the bronchopulmonary tree within 5 min making conventional radiography impossible, although good spot films could be obtained. Thickening agents, such as sodium carboxymethylcellulose and poly(vinylpyrrolidone) (PVP), were added to the cesium salt solutions to delay absorption and to slow their rate of passage.

Segmental bronchograms were performed on two patients with bronchogenic carcinoma using 30% CsCl formulated with 3% sodium carboxymethylcellulose. Radiopacity was good but the CsCl was absorbed from the tracheobronchial tree within 3 min and both patients complained of severe chest pain.

A CsCl solution (10 mL, 30%) was injected through the cervical os in dogs to evaluate its utility in uterine and fallopian tube imaging. Again, good roentgenograms were made and no obvious toxicities were noted. However, concerns regarding toxicity and acute pain in patients prevented further clinical investigation of this cesium salt.

D. Thorium

Thorium ($Z = 90$) is the heaviest metal (with the exception of uranium) that occurs naturally and is available in appreciable quantities. Its X-ray contrast enhancement potential was recognized early through the use of ThO_2 in pyelography[40] and bronchography.[41] The use of colloidal ThO_2 as an X-ray contrast agent became widespread after the demonstration in the late 1920s of its tremendous utility in cerebral arteriography by Moniz[42] and liver imaging by Radt.[43] As stable ThO_2 formulations had little acute toxicity and caused little discomfort to patients, they became widely used as X-ray contrast agents.[44] One well-known formulation was available commercially as Thorotrast. However, it is interesting to note that the American Medical Association did not endorse the use of Thorotrast because of its imperfect elimination from the body and its radioactivity.[45]

Thorotrast contained 25% (19−20 wt %) colloidal ThO_2 and dextrin (16−19%) to provide protective colloidal emulsion with methyl *p*-hydroxy benzoate (0.15%) added as a preservative. The average particle size was 3−10 nm (mean 5.5 nm). It was opalescent and odorless (with the consistency of heavy oil) and could be used as received or be diluted with glucose or a salt solution before use.

One estimate put the worldwide clinical use of Thorotrast at about 11 tons between 1928 and 1950, indicating that between 2.5 and 10 million people were exposed to the agent.[46] The majority of Thorotrast was consumed in Europe, North America, and Japan. While its main uses were angiography and liver imaging, it was used in practically every conceivable radiological contrast enhanced study of the time.[47−49]

A typical cerebral contrast angiography study required between 20 and 50 mL of Thorotrast, injected directly into the carotid artery. This proce-

dure was used in the diagnosis of brain tumors, abnormalities of encephalic arteries, and meningitis. Limb angiography required 20 mL of Thorotrast to demonstrate the location of thrombosis, embolism, and the development of collateral circulation. For liver imaging, three intravenous injections of Thorotrast (25 mL per injection) every other day were required.

Other uses of Thorotrast included imaging of the bladder and urethra. Local uses included visualization of body cavities such as sinus and fistula via instillation. In one instance, Thorotrast was even used in obstetrics. The lining and the shape of the placenta were demonstrated as were the number of fetuses present!

Although the direct injection of Thorotrast into the vein, artery, or body cavity was almost painless and produced few acute adverse reactions, extravasation did occur, especially when large amounts of Thorotrast were injected quickly.

Almost all systemically administrated ThO_2 was retained by the body. Uptake by the cells of the reticulendothelial system (RES) took place over a period of days and it remained there indefinitely. About 70% of the total ThO_2 body deposit was in the liver, 20% was in the spleen and the remaining 10% could be found in lymph nodes and bone marrow.[50−53]

Of course the toxicity of ThO_2 arose from its radioactive emission since the natural occurring isotope ^{232}Th is an α emitter (4.08 MeV, $t_{1/2} = 1.41 \times 10^{10}$ yr). The long-term exposure of tissues to radiation produced two sets of "side effects": malignant tumors such as hemangioendotheliomas and heptomas and fatal blood disorders such as leukemia and anemia. The latency periods for these conditions were extremely long. For example, on average, hemangioendothelioma occurred 25−30 years after the injection of Thorotrast. A recent Danish study on the long-term mortality of Thorotrast usage confirmed an excessive number of deaths were caused by the injection of Thorotrast. The leading causes of death were related to specific radiation effects such as carcinogenesis and liver cirrhosis.[54]

E. Tin

After Thorotrast ceased to be used as a contrast agent, new materials including colloidal stannic oxide were investigated as liver imaging agents.[55]

Colloidal suspensions of SnO_2 were prepared in concentrations of 10−20% w/v of tin. Particle size was generally less than 2 mm with most of the particles less than 1 mm, and the pH of these suspensions was around 7. Some preparations also contained 25% sucrose; these formulations were milky white and flowed freely.

An in vitro study compared the radiopacity of tin with that of thorium and iodine. Ten percent solutions (w/v) of tin-, thorium-, and iodine-containing materials were placed in identical tubes and inserted in the center of a Lucite phantom. Radiographs were taken at 40, 60, and 80 kVp. Tin was found to be highly radiopaque—at least equivalent to iodine and thorium at the X-ray energy levels investigated.

The potential of SnO_2 as a liver enhancing agent was demonstrated in a comparitive study with Thorotrast in rabbits and dogs. Thorotrast was given to the animals intravenously at a dosage of 1 mL/kg (∼ 200 mg of Th/kg; 0.86 mmol/kg), the maximum clinical Thorotrast dose for human use. A single dose of SnO_2 was about 350 mg of Sn/kg (2.95 mmol/kg). Some animals received more than one dose of tin with a 1−2 day interval between doses. With a single dose, liver and spleen were moderately well visualized by both SnO_2 and ThO_2: after multiple doses SnO_2 always proved to be superior to a single dose of ThO_2.

Both rabbits and dogs tolerated SnO_2 injections well even with repeated dosing. Maximum radiopacity of the liver and spleen was usually achieved in 4−6 h, and there was no demonstrable fading of this radiopacity even after 1 month. A long-term study in rabbits, rats, and dogs (up to 5 years) indicated that the long-term retention of SnO_2 particles was largely innocuous to animal tissues.[56] Gross and histological examination showed neither fibrosis nor neoplasia or any other evidence of interference with life processes. Despite its apparent physiological inertness, its imperfect excretion and long-term body retention precluded the clinical evaluation of the SnO_2.

Recently, SnO_2 was used to coat silica core particles in a sol−gel process. The resulting agglomerate-free, core−shell binary oxide particles contained about 13% SnO_2. The use of these particles as an X-ray contrast agent additive in composite materials, such as dental fillers, has been suggested.[57]

F. Zirconium

Insoluble ZrO_2 was proposed as a GI contrast agent as early as 1909 but was not used due to its taste and its expense. In 1955, a 25% aqueous suspension of ZrO_2 was investigated as an agent for liver imaging, although intravenous injection in animals consistently produced pulmonary infarction and death. Postmortem studies indicated that aggregation of ZrO_2 particles caused multiple pulmonary emboli. In addition, even though some ZrO_2 particles entered the reticuloendothelial cells in liver and spleen, contrast enhancement obtained on roentgenograms was not great.[58]

Despite its low atomic number ($Z = 40$), two in vitro phantom studies on aqueous solutions of zirconium glycolate, zirconium lactate, and sodium zirconyl citrate demonstrated that their radiopacity was not inferior to that of either iodine or barium at lower X-ray energies (between 30 and 50 kVp).[59,60] However, zirconium glycolate and zirconium lactate failed in a bronchography study, as the enhancement of the bronchogram was insufficient to provide satisfactory interpretation. Sodium zirconyl citrate failed as a contrast agent for cerebral angiography. It was concluded that in most procedures where X-ray energies of 70−90 kVp are used, the X-ray contrast enhancement produced by Zr compounds was inadequate.

Currently, ZrO_2 particles are used as X-ray contrast agent additives in cements for prosthetic fixation in ceramic-bearing total hip arthroplasties.[61]

However, the biocompatibility and physiological inertness of these particles are now being questioned.

G. Tantalum

Tantalum powder (particle size 2.5−5 mm) was investigated extensively as an X-ray contrast agent for bronchography in the late 1960s.[62−64] Some advantages over other agents of that time (iodine, and barium-based agents) were demonstrated in several in vitro and animal studies.[65−69] Tantalum caused little local irritation in the airways and lacked any known systemic toxicity. Since tantalum metal is highly radiopaque and has such a high density (16.6 g/mL), only a small volume of Ta powder (0.5−1 mL) was needed to obtain high-quality bronchograms. The powder coated airways evenly and did not interfere with normal pulmonary function. In addition to pure Ta powder, Ta_2O_5 powder was also tested in some bronchography studies.

Multicenter trials of tantalum powder as an X-ray contrast agent for tracheobronchography involved hundreds of patients with various respiratory symptoms. Pediatric applications were also investigated.[70] In general, Ta powder was introduced into patient's airways via a catheter which was attached to a reservoir of Ta powder.

Excellent tracheobronchograms with sharp demarcation of airway walls and fine mucosal detail were obtained with about 0.5 mL (8 g) of Ta powder. Anatomical structures (to 1 mm in diameter) of the tracheobronchial tree were clearly visualized. Abnormalities caused by stenosis, lesions, bronchogenic carcinoma, and other pathologies were clearly delineated. Ta powder was generally cleared from patients by coughing within 24 h. However, one clinical trial demonstrated that although Ta powder that deposited in the trachea and major bronchi cleared out quickly, Ta powder deposited in distal bronchioles cleared much more slowly and the Ta powder deposited in the terminal regions did not clear at all.[71]

Using ^{182}Ta as a radioactive tracer, the clearance of Ta powder following bronchography was investigated in dogs.[72,73] Long retention of Ta powder (up to 20% of the initial dose and up to 205 days) in the lung was confirmed. In other animal studies using Ta and Ta_2O_5 powders, high incidences of pneumonia and inflammatory responses were observed.[74] Due to these concerns, the use of Ta powder in bronchography did not progress beyond clinical trials.

Tantalum powder and tantalum pentoxide powder were also investigated briefly as agents for liver imaging.[49] Fresh suspensions of Ta powder (50 g of Ta in 200 mL of 15% sorbitol) were intravenously injected into rats and dogs.[75] A high degree of radiopacity was developed in the liver and spleen within days and persisted for 4−6 weeks. The lymph nodes at the hilus of the liver became radiopaque within 5−14 days. These nodes remained radiopaque for 2−3 months, then gradually lost their radiopacity.

The potential utility of Ta powder and Ta_2O_5 as agents for GI imaging was demonstrated in animal studies. Insufflation of Ta powder to the esophagus produced clinically useful images,[76,77] and oral administration of an aqueous suspension of Ta powder yielded useful films of the stomach.[78] In one report, testing of Ta powder extended to angiography. Intravenous injection of tantalum particles to dogs produced an image of an intravascular clot.[79]

Tantalum powder is currently under investigation as the X-ray contrast component of embolic agents intended for the treatment or preoperative embolization of hypervascular tumors.[80,81]

H. Tungsten

Investigations into the use of tungsten-containing materials as contrast agents for bronchography were carried out in parallel with the studies of tantalum compounds.[66,74] Tungsten powder (7.2 mm average size), $CaWO_4$ powder (5−6 mm), and a suspension of $CaWO_4$ (1 g in 10 mL of reconstituted human serum albumin) were studied in animals. Good radiological images of the respiratory passages were obtained, particularly for those airways greater than 1 mm in diameter. However, they were not superior to images obtained using Ta powder.

Tungsten powder is currently used as an X-ray contrast agent additive in embolic agents used in the treatment and preoperative embolization of hypervascular tumors.[80,81] As an added benefit, the dark color of W powder provides a good visual guide to surgeons (who can easily distinguish cancerous from healthy tissues by their differential tissue staining) permitting a more complete removal of the tumor.[80]

I. Rare Earth Elements

Formulations of insoluble oxides of cerium, gadolinium, and dysprosium with stabilizers have been investigated as CT contrast agents.[26,31] It was hoped that these particulates would target the cells of the RES to provide contrast enhancement in the liver and spleen.

To prepare formulations of these insoluble particulates, they first have to be coated with a stabilizer. CeO_2 solid was suspended in 0.2% gelatin and sonicated and then centrifuged. It was reconstituted with water to form a solution with 200 mg of CeO_2/mL and 5.66% gelatin.

Gd_2O_3 and Dy_2O_3 were suspended in 0.33% PVP-40 and prepared in the same manner to provide final formulations of 200 mg of Gd_2O_3/mL in 2.74% PVP-40 and 200 mg of Dy_2O_3 in 2.61% PVP-40.

Formulation particle size was measured using light microscopy. Over 90% of the particulates were 2.5 mm or smaller. However, aggregation of the particles occurred when they were mixed with human plasma. Aggregates larger than 25 mm were detected in the CeO_2 (gelatin-coated) formulation while less than 10% of the particles were larger than 10 mm in Gd_2O_3 and Dy_2O_3 formulations. All three formulations were administered to rabbits intravenously to test their potential utility as hepatobiliary CT contrast agents. At doses of 0.5 or 1.0 g per animal, contrast enhancement of rabbit liver of 150 and 300 HU was achieved. In tumor models (V2 carcinoma), normal liver tissues enhanced similarly while tumor tissue displayed significantly lower opacification. CT images of a

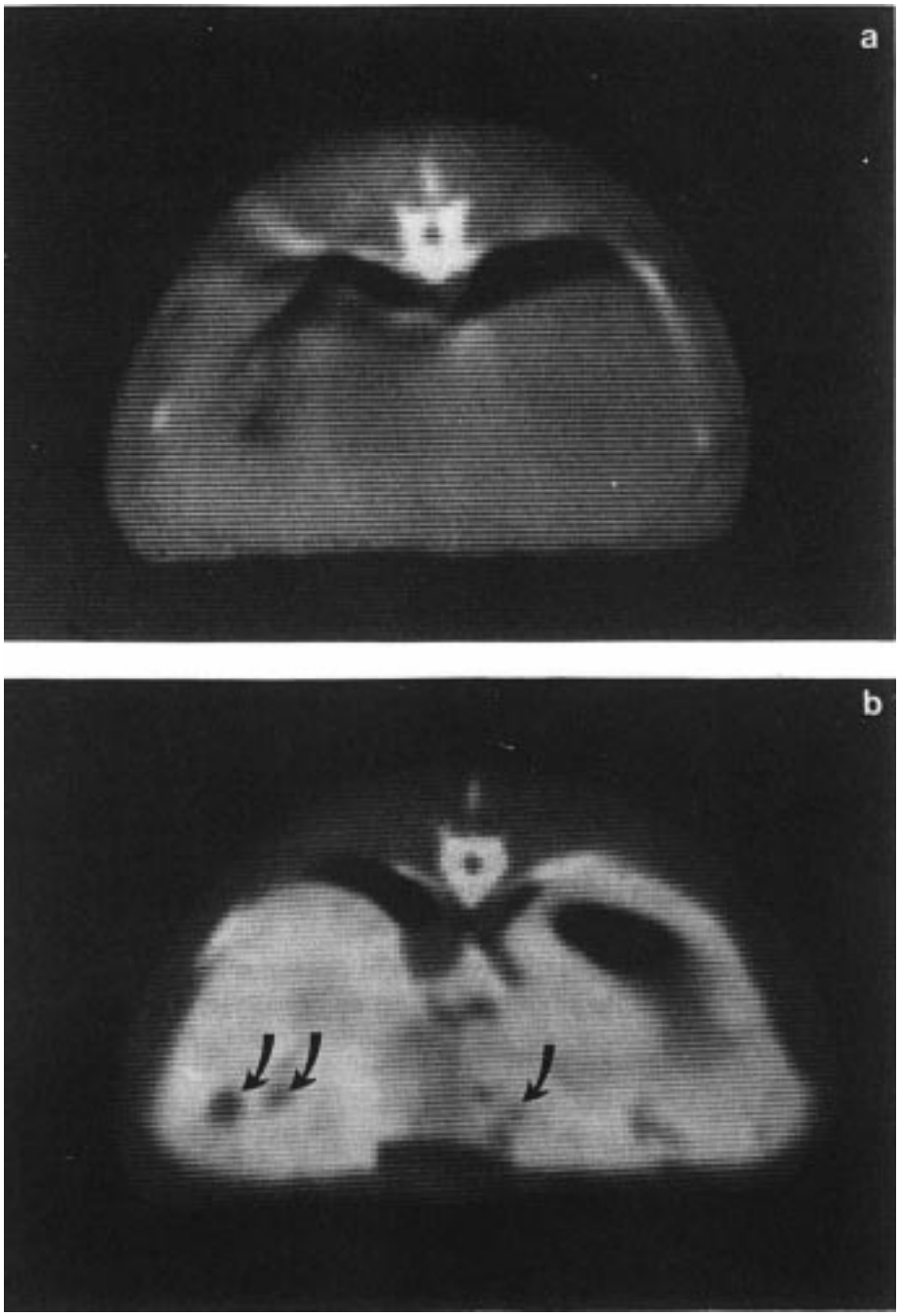

Figure 6. CT images of a rabbit abdomen. (A) Before contrast, liver CT number is 50 HU. (B) Sixty minutes after intravenous injection of Gd_2O_3 particles. Liver is brightly opacified (250 HU). Implanted tumor nodules (arrows), up to 5 mm in diameter, stand out as filling defects (31 HU). The nodules are much more easily seen after contrast administration. (Reproduced with permission from ref 26b. copyright 1981 Elsevier Science.)

rabbit abdomen are shown in Figure 6. The comparison of tumor visibility pre- and postcontrast is striking.

The difference in CT radiopacity (measured in HU) between normal liver and tumor (D_{l-t}) is a measure on the visibility (contrast) of the tumor. The mean D_{l-t} prior to contrast agent administration was 24 HU. Within 5 min of postinjection of rare earth oxides (1 g/per animal), the average D_{l-t} reached 162 HU. This maximum differential radiopacity lasted for at least 1 h, which allowed the detection of tumors approximately 5 mm in diameter. In comparison, the maximal D_{l-t} for a soluble iodinated agent (Renografin) is about 77 HU, 20 s after injection, followed by a gradual decline as the enhancement of normal tissue falls due to its rapid clearance and excretion.

In healthy rabbits, the liver uptake of rare earth oxide particles was complete within 1 h, although about 95% of the injected dose remained in the liver. Formulations containing radioactive rare earth oxides were injected into healthy rats to study their biodistribution and clearance. At 1 h, more than 90% of the injected dose was taken up by the liver and spleen. Over time some of the material was released by liver and deposited in bone. At 21 days, about 25% of the injected dose of dysprosium and gadolinium was found in bone, compared to 5% of the injected cerium. For all three agents, the amount of material

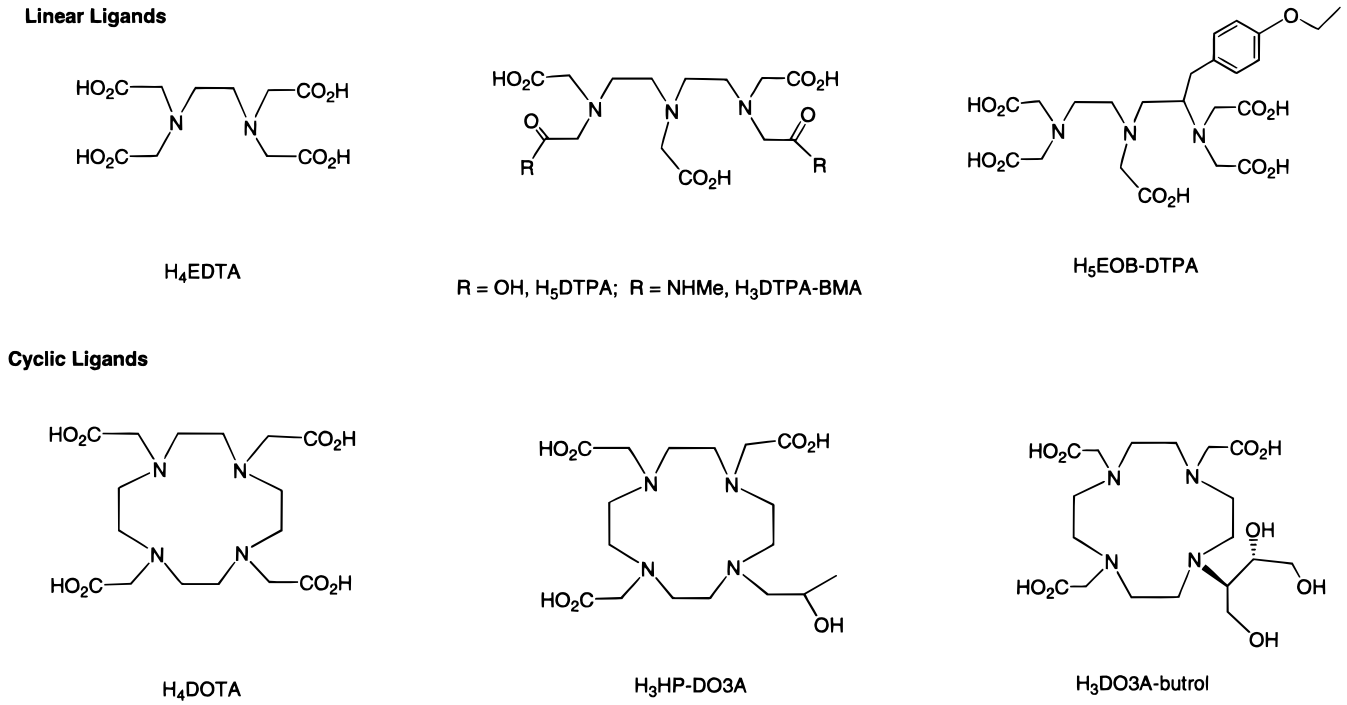

Figure 7. Representative chelating agents (I).

remaining in the animals after 21 days exceeded 80% of the injected dose.

The intravenous LD_{50} for CeO_2 was determined to be 5.4 g of Ce/kg in mice, which is about 10−20 times the effective imaging dose (0.4 g/kg). Animals receiving the imaging dose during the CT studies showed no visible signs of acute toxicological or pharmacological distress. However, safety concerns, in light of the long body retention and tendency for bone uptake, as well as their high costs prevented clinical investigation of these agents.

In summary, due to their poor elimination profiles and both acute and long-term toxicity issues, there are no X-ray contrast agents based on metal salts or particulates (other than $BaSO_4$) currently approved for human use and there is little active clinical research interest in this field. Recently, an intravenous liver agent consisting of iron oxide particles has been approved for MRI. However, unlike the heavy metals already described, iron is an essential element for human metabolism and incomplete elimination of iron oxide particles is acceptable so long as the resulting iron concentration does not exceed the daily body burden of iron. The metabolism of iron cells in the RES is slow (on the order of days) and the metabolized iron enters the physiological iron pool.[82]

IV. Heavy Metal Complexes as X-ray Contrast Agents

A metal chelate complex is a coordination compound of a metal ion with a chelating agent (often an organic ligand). An important property of a chelating agent is its ability to alter the behavior of the metal ions it binds in biological systems. The biodistribution and excretion profile of a heavy metal ion will be markedly modified upon chelation: in general, a chelating agent will lower the in vivo absorption of a heavy metal ion. A chelating agent that is hydrophilic, such as EDTA or DTPA (see Figure 7), usually will increase the proportion of its metal complex excreted through the renal system and accelerate the excretion of the complexed metal ion from a biological system. Conversely, a lipophilic chelating agent such as EOB-DTPA (vide infra) results in its metal complexes being taken up by the liver and bile and excreted fecally.

The toxicity of a heavy metal ion, which is the manifestation of its collective interactions with a biological system, may also be profoundly impacted by chelation and is often reduced significantly. This has led to the development of chelating agents as therapeutic drugs to treat heavy metal poisoning; in fact, lead poisoning in children has been successfully treated with intravenous EDTA administration since 1952.[83]

The successful development of metal-containing MRI contrast agents and radiopharmaceutical imaging agents over the past two decades has significantly benefited from and contributed to progress in the design and synthesis of biocompatible chelating ligands.[84,85] Several commonly used chelating agents are listed in Figure 7, together with their usual abbreviations. All of the chelating agents in Figure 7 belong to the family of polyaminopolycarboxylate ligands, not surprising since hard donor atoms such as oxygen and nitrogen will form strong coordinate bonds to hard metal ions such as lanthanide metals.

One parameter used to describe these complexes is the thermodynamic stability constant K which, for an equilibrium $ML \rightleftharpoons M + L$ is

$$K = [ML]/[M][L] \quad (8)$$

Table 4. Thermodynamic Stability Constants and LD_{50} (Mice) Data for Selected Metal Complexes

complexes	log *K*	LD_{50}
$(NMG)_2GdDTPA$	22.4	6−10
$Na_2YbDTPA$	22.6	10 (rat)
GdDTPA-BMA	16.9	14.8
(NMG)GdDOTA	25.8	11
GdHP-DO3A	21.8	12
GdDO3A-butrol	23.8	∼30
$(NMG)_2GdEOB-DTPA$		7.5
(NMG)GdEDTA	17.3	0.3
$Na_2PbEDTA$	18.1	∼1.5 (rabbit)
$Na_2BiDTPA$	27.8	<1.4 (dog)

Table 4 lists selected thermodynamic stability constants for a number of polyaminopolycarboxylate ligands. In general, since the toxicity of the free metal ion is greater than the toxicity of its chelate complex, the stability constant can be a useful predictor of the toxicity of the complex. However, there are many other factors that profoundly influence toxicity, such as local physiological factors (pH and temperature), the presence of endogenous chelating agents (proteins, citrate, carbonate, etc.), and other endogenous metal ions which can be kinetically favored to undergo in vivo exchange and transmetalation. A modified form of the stability constant, the selectivity constant (K_{sel}), has been defined as a quantitative measure of the affinity of a metal ion to bind to a chelating agent in the presence of other metal ions and chelating agents at a given pH. K_{sel} appears to be a superior predictor of metal chelate complex toxicity and has been shown to correlate linearly with acute toxicity.[85]

There are two types of polyaminopolycarboxylate chelating agents—the linear structures, which include EDTA and DTPA and their derivatives, and cyclic forms which include DOTA and DO3A and their derivatives. The simple stability constants (*K*) of these cyclic and linear chelating agents complexed with Gd (III) do not differ greatly, as shown in Table 4. However, the kinetics of their metal complex formation and complex dissociation behavior are markedly different. Formation rates of metal complexes with cyclic chelating agents are typically slow and their rates of dissociation are slow as well. Hence, heavy metal complexes incorporating cyclic chelates usually demonstrate superior kinetic stability.[86,87]

The syntheses of the metal complexes encountered in this section are typically well established and straightforward. Metal incorporation can be achieved through simple reactions of metal oxides or halides with the desired ligand. However, the large-scale synthesis of macrocyclic chelating agents has presented a significant industrial challenge.[88]

A. GdDTPA and YbDTPA

GdDTPA, formulated with meglumine (*N*-methyl glucamine, NMG) as a counterion, became the first metal complex to be approved for use as a contrast agent for MRI (gadopentetate dimeglumine, Magnevist). It is available commercially as a 0.5 M solution, and the recommended human dosage is 0.1 mmol/kg.

The first testing of $(NMG)_2GdDTPA$ as an X-ray contrast agent in humans occurred serendipitously, almost paralleling the first human experience with iodinated contrast agents.[89] After a patient received $(NMG)_2GdDTPA$ in an MRI procedure, a subsequent unenhanced CT scan of the pelvic and abdominal region revealed unexpected X-ray contrast enhancement in the urinary tract. Follow-up studies on another human subject indicated that $(NMG)_2GdDTPA$ provided a contrast enhancement equivalent to that of 5 mL of iodinated contrast media (282 mg of I/mL). Subsequent phantom studies demonstrated greater attenuation by $(NMG)_2GdDTPA$ solutions compared with equimolar iodine solutions at higher tube voltages (around 120 kVp). Iodinated agents contain three iodine atoms per molecule and can be formulated as more concentrated solutions—it was calculated that it would take double or triple volumes of 0.5 M $(NMG)_2GdDTPA$ (i.e., 130 mL for a 70 kg human) to produce equivalent X-ray contrast enhancement compared to iodinated agents (300 mg of I/mL).[90]

YbDTPA was investigated as an intravascular CT agent in 1986.[91] Phantom scans of equal weight concentrations YbDTPA and an iodinated agent at 96 kVp showed ytterbium to be slightly more radiodense. However, at 125 kVp, ytterbium was much more radiodense than iodine. Intravascular injection of 180 mg of Yb/mL solutions in dogs demonstrated Yb's utility as an X-ray contrast agent. On CT scans, identical volumes of YbDTPA caused greater opacification of the mediastinal vessels than iodine (180 mg of I/mL). In pulmonary angiography, YbDTPA gave visibly denser opacification and better delineation of the right pulmonary artery and its branches than iodine. Dynamic scans of dogs receiving increasing doses of YbDTPA and iodinated agents showed ytterbium was denser in the aorta and inferior vena cava than iodine in terms of maximal change in Hounsfield units on an equal weight basis. The time−density curve showed ytterbium was denser than iodine, and the shape of the curve followed the same pattern as iodinated agents, indicating that YbDTPA pharmacokinetics are similar to those of typical iodinated agents.

Additional phantom and animal studies confirmed that at equimolar concentrations, both $(NMG)_2$-GdDTPA and YbDTPA are superior to iodine in producing CT enhancement at 120 and 137 kVp.[92] At a dose of 0.5 mmol/kg in dogs, the opacification of the aorta was significantly higher with $(NMG)_2$-GdDTPA than with iodine (197 vs 157 HU). Enhancement of the liver was also visible (21 vs 12 HU), and the enhancement obtained with YbDTPA was similar to that seen with $(NMG)_2GdDTPA$. In addition, for all three agents, the mean time to peak enhancement in aorta and liver were similar, again demonstrating similar pharmacokinetic profiles.

The easy availability of $(NMG)_2GdDTPA$ for human studies has made additional investigations possible with this agent. There are two principal driving forces for radiologists to test $(NMG)_2GdDTPA$ (approved as an MRI contrast agent) as an X-ray contrast agent. First, some patients are contraindi-

cated for iodinated agents based on allergic reactions or renal insufficiency.[93] Second, since heavy metals such as Gd and Yb have higher K edges than iodine, they will produce better contrast enhancement than iodine at higher X-ray photon energies, potentially reducing radiation exposure to the patient.

Initial investigations into the use of $(NMG)_2$-GdDTPA as a CT contrast agent yielded unconvincing results. In one experiment, abdominal or thoracic CT scans were performed on patients contraindicated for iodinated agents before and after the administration of 0.2 mmol/kg $(NMG)_2$GdDTPA: no visible improvement was observed in the contrast-enhanced scans.[90] In another experiment, CT scanning immediately following $(NMG)_2$GdDTPA-enhanced MRI scanning showed no liver enhancement and only a slight contrast enhancement of the renal cortex. However, time-delayed images of the kidney and bladder demonstrated a high degree of contrast.[94] A third experiment demonstrated that the presence of $(NMG)_2$GdDTPA in the renal collection system varies greatly among patients after administration of a standard dose (0.1 mmol/kg) for MRI.[95] The degree of X-ray contrast enhancement cannot be reliably predicted from the time of intravenous injection, from the patients' weight, or from simple indices of renal function. The utility of $(NMG)_2$GdDTPA as a CT contrast agent was finally demonstrated at a dose of 0.5 mmol/kg in a cranial CT experiment in which satisfactory vascular enhancement was obtained after a 90 kg volunteer received 90 mL of *iv* $(NMG)_2$-GdDTPA.[96]

More recently, $(NMG)_2$GdDTPA has found use in DSA in patients with renal insufficiency or allergy to iodinated agents.[97−100] Although the contrast was less marked than with iodinated agents, most of these procedures yielded adequate diagnostic information using $(NMG)_2$GdDTPA doses below 0.3 mmol/kg. Intraarterial use of $(NMG)_2$GdDTPA was also well-tolerated by patients. Renal function remained stable for patients with renal insufficiency, and there were no allergic reactions among patients who were believed to be hypersensitive to iodinated agents.

The use of $(NMG)_2$GdDTPA as an X-ray contrast agent in conventional and interventional radiology has also been reported.[101] Conventional procedures performed with 20−45 mL of $(NMG)_2$GdDTPA (0.5 M) included urinary tract and bladder imaging and biliary tree imaging. Interventional procedures included percutaneous nephrostomy (creation of an artificial port draining the kidney) and biliary tract drainage. Image quality, albeit inferior to that obtained using iodinated contrast agents in all cases, was at least of diagnostic utility in all cases.

$(NMG)_2$GdDTPA distributes rapidly and completely throughout the extracellular fluid compartment once administered. Its plasma half-life is about 15 min, and it is excreted principally by the kidneys with an elimination half-life of about 94 min—overall, the pharmacokinetic profile of $(NMG)_2$GdDTPA is similar to that of iodinated agents.[102]

At 0.1 mmol/kg, the administration of $(NMG)_2$-GdDTPA causes little discomfort to patients and few adverse drug-related reactions (0.025%). Patients with renal insufficiency demonstrate good renal tolerance to $(NMG)_2$GdDTPA, and it has been shown to be less nephrotoxic than idinated agents.

B. GdDTPA-BMA

GdDTPA-BMA (gadodiamide, Omniscan) is another approved MRI contrast agent (prepared from a linear chelating agent DTPA−bis(methyl)amide). The ligand contains only three anionic carboxylate groups, which results in a neutral (nonionic) complex with Gd(III). GdDTPA-BMA provides a low osmolar (790 mOsm) solution when compared with $(NMG)_2$GdDTPA (1940 mOsm).

The pharmacokinetic and biodistribution profile of GdDTPA-BMA is similar to that of $(NMG)_2$-GdDTPA.[103] It is an extracellular agent and is rapidly excreted renally with an elimination half-life of around 70 min. When formulated with 5 mol % CaDTPA-BMA, its LD_{50} in mice is 34 mmol/kg, providing a safety margin of 340 at the commonly used dosage of 0.1 mmol/kg.

A CT phantom study demonstrated that GdDTPA-BMA produced the same level of X-ray contrast enhancement to that of $(NMG)_2$GdDTPA at the same concentration. However, at 0.5 M, its X-ray contrast enhancement is only 36% of that of iodinated agents at (300 mg of I/mL), the same as for $(NMG)_2$GdDTPA.[90]

At a dose of 0.2 mmol/kg, the first CT scans of thoracic and abdominal regions in patients did not prove to be clinically useful. Sufficient liver parenchymal enhancement was not achieved.

An investigation of the use of GdDTPA-BMA as an X-ray contrast agent in arterial angiography was modestly successful.[104] A total of 15 patients were examined with both GdDTPA-BMA and an iodinated agent. The X-ray tube voltage was 110 kVp for angiographic procedures using GdDTPA-BMA (40 mL of 0.5 M) and 75 kVp in the procedures using relatively diluted iodinated agents (40 mL of 150 mg of I/mL). In all but one case, diagnostically useful information was obtained with GdDTPA-BMA. However, the images were all of poorer quality than the images produced using the iodinated agent (an example is shown in Figure 8), although the investigators claimed that a significant reduction in radiation exposure was achieved by using gadolinium agents instead of iodinated agents. On average, an imaging procedure using an X-ray source at tube voltage of 110 kVp reduces the patients' overall radiation dose greater than 3-fold compared to a 75kVp procedure.

Another investigation demonstrated the utility of GdDTPA-BMA as an X-ray angiographic agent in the diagnosis and treatment evaluation of renal artery stenosis in patients with renal insufficiency.[105] Twenty-four patients underwent intraarterial DSA using GdDTPA-BMA and CO_2 as contrast media for diagnosis and percutaneous renal intervention. When compared with CO_2 (CO_2 gas provides X-ray contrast enhancement by removing dense body fluids from an anatomical region and is an example of negative contrast) angiograms, the images produced by Gd-

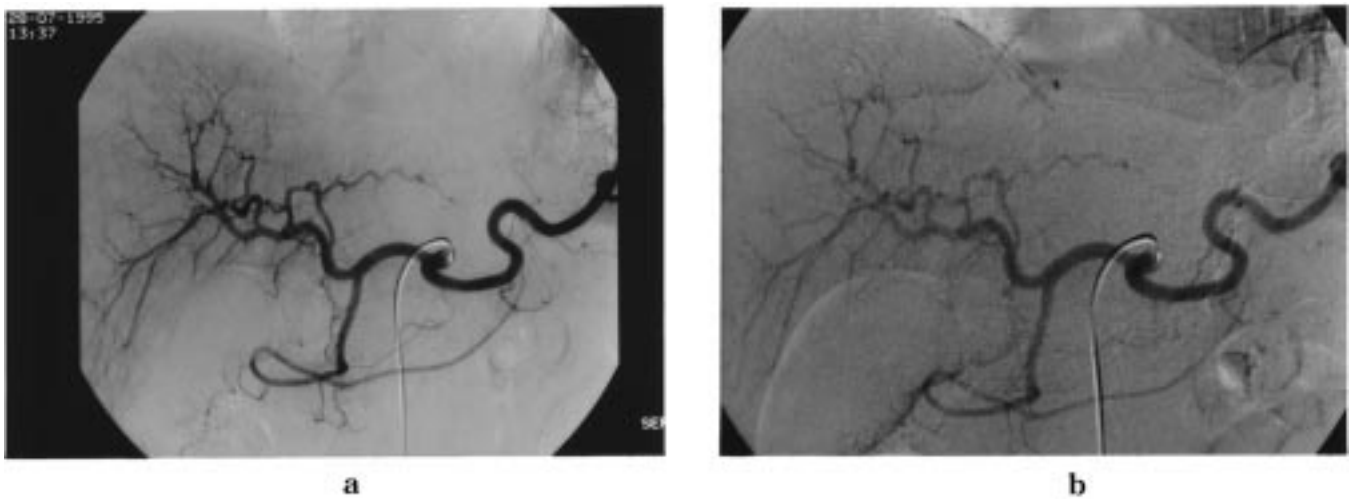

Figure 8. Selected angiogram of the celiac trunk and portal system in a patient. (A) Arterial phase with 75 kVp and iodine (300 mg I/mL) as the contrast agent. (B) Arterial phase with 110 kVp and GdDTPA-BMA (0.5 M) as the contrast agent. Although the image contrast with GdDTPA-BMA and the visualization of the small vessels is poorer than the image taken with the iodinated agent, it is adequate for diagnosis. (Reproduced with permission from ref 104. Copyright 1996 Springer-Verlag.)

DTPA-BMA depicted renal artery occlusions and provided far better delineation of the renal vessels.

C. GdHP-DO3A and GdDO3A-butrol

GdHP-DO3A (gadoteridol or ProHance) is another FDA approved MRI contrast agent. GdDO3A-butrol (gadobutrol, Gadovist) is another, related, MRI agent currently in clinical trials.[106] They are both neutral (nonionic) gadolinium (III) chelate complexes formed by cyclic chelating agents.

The use of GdDO3A-butrol as a contrast agent for CT was evaluated in vitro and in vivo (a rabbit model) and compared with iodinated agents.[107] Phantom measurements using spiral CT at increasing energy levels with this complex revealed that X-ray attenuations for gadolinium were 18.1% (80 kVp), 38.2% (120 kVp), and 40% (137 kVp): higher than those of iodine at mass equivalent concentrations.

Increasing doses of GdDO3A-butrol and an iodinated agent were administrated as bolus injections into the ear vein of rabbits. Dynamic scans were carried out prior to injection and continuously postinjection, and X-ray contrast enhancement, measured in HUs, was then calculated for each ROI. The mean peak enhancements in the aorta for the gadolinium agent were 216, 313, and 591 HU for doses of 0.7, 1.0, and 1.5 mmol of Gd/kg while for the iodinated agent 224 and 498 HU for doses of 1.0 and 2.4 mmol of I/kg. It was concluded that the mean peak enhancements of GdDO3A-butrol (1.5 mmol Gd/kg) produced a similar degree of X-ray contrast enhancement to that provided by a larger dose of the iodinated agent (2.4 mmol/kg).

Clinical experience with this class of compounds as X-ray contrast agents has focused on studies with the commercially available GdHP-DO3A. One study compared the ability of GdHP-DO3A and iohexol to detect brain tumors by CT.[108] GdHP-DO3A crossesthe disrupted blood-brain barrier just as iodinated agents do, and the degree of contrast enhancement with GdHP-DO3A was within 20% of that of the iodinated agent. It was concluded that GdHP-DO3A is a viable alternative contrast agent for CT.

Another research study evaluated the use of GdHP-DO3A as an alternative to iodinated agents in lower extremity DSA.[109] Fifteen patients received 20−24 mL (0.5 M) of GdHP-DO3A by intraarterial (*ia*) injection. DSA images of the calf were obtained by using a 3 mm aluminum filter to increase the mean X-ray photon energy. Similarly, DSA images were acquired with an iodinated contrast agent. Segmental stenosis and occlusion were diagnosed with good sensitivity and specificity using GdHP-DO3A. It was concluded that intraarterial administration of GdHP-DO3A is safe and may be used for DSA in patients contraindicated for iodinated agents. However, the imaging technique had to be modified to accommodate the higher K edge of gadolinium.

The pharmacokinetic profiles of GdHP-DO3A and GdDO3A-butrol are similar to that of $(NMG)_2$-GdDTPA.[106,110] Once injected, they rapidly distribute from the vascular compartment to the extracellular fluid space and are predominately excreted through the renal system with a half-life of around 90 min. In all cases, more than 90% of the injected dose is recovered in the urine within 24 h.

Animal studies demonstrated reduced acute toxicity for both GdHP-DO3A and GdDO3A-butrol compared to that of $(NMG)_2$GdDTPA. Both agents were well tolerated in healthy volunteers at dosages up to 0.3 mmol/kg for GdHP-DO3A, but GdDO3A-butrol was well-tolerated at an even higher dosage of 0.5 mmol/kg. Coupled with its high solubility, which permits its formulation as a concentrated one molar solution, GdDO3A-butrol may be developed as an alternative X-ray contrast agent that offers enhancement comparable to iodinated agents.

D. Ethoxybenzyl DTPA (EOB-DTPA) Complexes

GdEOB-DTPA is currently in the late stages of clinical testing as an MRI contrast agent for the liver and spleen.[111] The addition of a lipophilic ethoxybenzyl group to the carbon backbone of DTPA profoundly alters the pharmacokinetic and biodistribution properties of $(NMG)_2$GdDTPA. Following *iv* administration, GdEOB-DTPA rapidly distributes into the extracellular fluid space. However, unlike $(NMG)_2$-GdDTPA, which is exclusively excreted through the kidneys, between 30% and 70% of GdEOB-DTPA (depending on the species) is taken up by hepatocytes during its short plasma residence time through a so-called organic anion plasma membrane transport system to provide clinically useful MRI and X-ray contrast enhancement of the liver and spleen before being fecally excreted.[111e] In human volunteers, the apparent serum half-life of GdEOB-DTPA was about 2 h. At lower dosages (0.1 and 0.2 mmol/kg), the complete excretion of GdEOB-DTPA was divided evenly between urinary (within 12 h) and fecal (within 6 days) routes. On the other hand, at higher dosages (0.35 and 0.5 mml/kg), there is a significant increase in urinary elimination with a parallel decrease in fecal elimination, indicating some degree of saturation of the hepatocyte uptake transport system in the hepatobiliary disposition of GdEOB-DTPA (a phenomenon previously observed in small animals).

On the basis of the observed unique hepatocellular uptake, [M]EOB-DTPA complexes with a range of heavy metal elements, M = La, Ce, Pr, Gd, Dy, Yb, Lu, Pb, and Bi, were investigated as liver-specific agents for CT studies.[112] A phantom CT measurement at 137 kVp revealed that the molar X-ray attenuation of the [M]EOB-DTPA complexes was greater by a factor of 1.8 for Gd and 2.2 for Yb relative to iodine.

In a rat study all of the [M]EOB-DTPA complexes exhibited biliary excretion after intravenous injection of 0.5 mmol/kg. Biliary elimination ranged from 49% to 61%. In tumor-bearing rats a mean increase of 16 HU (10 min after injection) was observed for normal liver tissues whereas there was practically no enhancement for tumor tissue.

Further animal studies of GdEOB-DTPA[113a] and DyEOB-DTPA[113b−d] demonstrated that they may be suitable and well tolerated contrast agents for liver CT imaging. In rabbits with VX2 tumor implants, good visualization of lesions (3−20 mm in size) was provided using 0.5 mmol/kg doses of DyEOB-DTPA and 0.7 mmol/kg doses of GdEOB-DTPA. Tumor detection appeared to be at least as good as CT examinations using a nonionic iodinated agent.

A clinical investigation evaluated the efficacy and safety of GdEOB-DTPA as a liver-specific CT contrast agent in 15 patients with liver metastases.[114] Three dosages were studied: 0.2, 0.35, and 0.5 mmol/kg. Contrast enhancement increased with dose, and maximal liver enhancements of 13, 27, and 34 HU, respectively, were measured. Visualization of lesions improved for all dosages compared to unenhanced CT scans; however, only at the higher doses (0.35 and 0.5 mmol/kg) were liver enhancement, liver-to-tumor attenuation differentials, and tumor visualization graded as moderate or better.

The acute toxicity (measured as LD_{50}) was about 10 mmol/kg in mice for both YbEOB-DTPA and GdEOB-DTPA. In rats, LD_{50} was 7.5 mmol/kg for Yb, Pr, Gd, Dy, and LuEOB-DTPA. However, LD_{50} was only 3.5 mmol/kg for CeEOB-DTPA and 5 mmol/kg for BiEOB-DTPA. The concentration of metals or [M]-EOB-DTPA in bones is another indicator of the potential chronic toxicity of these metal complexes. Six hours after iv administration of [M]EOB-DTPA 0.5 mmol/kg in rats, bone concentrations of La, Ce, Pr, Pb, and Bi or their EOB-DTPA complexes were much higher than that of Gd, Dy, Yb, and Lu or their EOB-DTPA complexes.

E. Miscellaneous Metal Complexes

PbEDTA along with other metal complexes (incorporating Cd, Zn, Co, Ni, Ba, and Ce as metal ions with EDTA or EDTA-derivatized chelating agents) were investigated in the 1950s as X-ray contrast agents.[39b,115−117] In vitro phantom studies compared with iodine demonstrated marked X-ray opacity, and in animal studies useful X-ray images were obtained. An investigation using PbEDTA as an X-ray contrast agent was conducted on human subjects.[118] It was administered orally, intravenously, or intranasally. Diagnostically useful images were obtained in all cases. However, biodistribution studies in animals indicated a small amount of Pb failed to be eliminated (retained mostly in liver and bone). In addition, the safety margins were small between the effective dose and LD_{50}.[119] It was rapidly concluded that PbEDTA was not suitable for human use. Metal−EDTA complexes generally exhibit a low-level in vivo stability due to metal release which is caused by the competition from better in vivo chelating agents such as citrate, etc. However, it should be noted in the case of Pb that the toxicity profiles of its DTPA and diaminocyclohexanetetracetate complexes are no better than those of PbEDTA.[116]

BiDTPA (at a 1.12 M concentration) was evaluated in dogs to explore its potential utility as a bronchography or angiographic agent.[120] It was delivered to the right pulmonary bronchus via catheter for bronchography and was injected *iv* for angiography. Diagnostically useful bronchograms and angiocardiograms were obtained in both cases. Animals tolerated BiDTPA within the dosing limits of the bronchography study; however, many did not fare so well during the angiography procedure. Simultaneous administration of CaDTPA did not lower the acute toxicity of BiDTPA. Pulmonary and renal lesions attributable to BiDTPA were demonstrated in both procedures.

Recently, sodium bismuth tartrate, together with 2 equiv of dimercaptosuccinic acid (DMSA, a detoxifying agent), was evaluated as an in vivo X-ray contrast agent.[121a] At a concentration of 1.8 g/mL, bismuth tartrate produced an X-ray contrast enhancement comparable to an iodinated agent (Urografin, 370 mg of I/mL). This concentration was 18 times that of the LD_{50}, even in the presence of DMSA. Without DMSA, bismuth tartrate quickly concentrates in the liver, kidney, and spleen and then

discharges in bile. In the presence of DMSA, however, bimuth tartrate was quickly dissipated from the blood and accumulation in other tissues was minimal. Since bismuth tartrate is too toxic and its solubility is so low, additional work is needed to make its use as an X-ray contrast agent feasible. In addition, it should be noted that the sodium bismuth tartrate used in this study was poorly characterized—it is likely that upon addition of DMSA, BiDMSA complexes were formed. A recent study has demonstrated a thermodynamic preference of bismuth for thiolate ligation and all bismuth thiolate complexes invariably gave a yellow color,[121b−d] although the original investigator noticed a color change with the addition of DMSA.

V. Metal Cluster Complexes as X-ray Contrast Agents

Metal cluster compounds contain two or more metal atoms and involve substantial metal−metal bonding. A heavy metal cluster can provide significant X-ray attenuation within a relatively small molecular volume, much like triiodobenzene-based compounds. As X-ray contrast agents, these materials have two potential advantages: first, the higher degree of X-ray attentuation per molecule allows preparation of highly concentrated solutions with greater radiodensity than those currently attainable (or conversely, low-osmolality and low-viscosity formulations matching current levels of radiodensity could be prepared); second, the high-energy X-rays needed for the optimal use of these agents would result in a reduced radiation dose to the patient.

Unfortunately, most metal cluster compounds are either unstable or insoluble in water, thereby preventing their use in medical applications. It is possible, however, to impart water solubility and stability through chelation of these metal clusters by using inter- and intramolecular ligand systems. The central challenge facing the chemist in the research and development of metal cluster-based X-ray contrast agents is to identify the right chelation systems. The resultant cluster complexes have to be nontoxic, stable under physiological conditions (temperature, pH, and the presence of competing ligands and metal ions) and completely excreted within a reasonable time frame.

Two commercially available chelating agents used successfully to stabilize and solubilize metal cluster systems are shown in Figure 9.

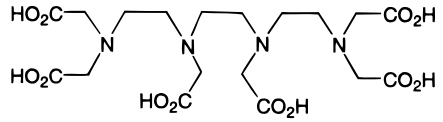

H_6TTHA

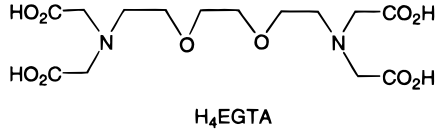

H_4EGTA

Figure 9. Representative chelating agents (II).

A. Tungsten Cluster Compounds

Among heavy metals ($Z > 50$), aqueous tungsten cluster chemistry has received considerable attention. Several reviews describe sulfur-bridged tungsten clusters,[122] and this group of metal clusters have served as excellent leads for the development of prototypical heavy metal cluster-based X-ray contrast agents.[123]

1. Dinuclear Tungsten Cluster Compounds

$Na_2[W_2O_4(EDTA)]$, a white solid with an aqueous solubility of 0.5 M at pH 7, was prepared according to literature methods.[124,125] The $[W_2O_2S_2(EDTA)]^{2-}$ anion was obtained through the reaction of EDTA with the aqua ion, $[W_2O_2S_2(H_2O)_6]^{2+}$, which in turn was obtained as a byproduct from the reduction of $(NH_4)_2[WS_4]$ in HCl.[126,127] The solubilities of $Na_2[W_2O_2S_2(EDTA)]$ and $(NMG)_2[W_2O_2S_2(EDTA)]$ are 75 and 500 mM, respectively.

Orange crystals of $Na_2[W_2O_2S_2(EDTA)]$ were obtained by slow evaporation of an aqueous solution and the structure determined by X-ray crystallography.[128] Figure 10 is an ORTEP drawing of the

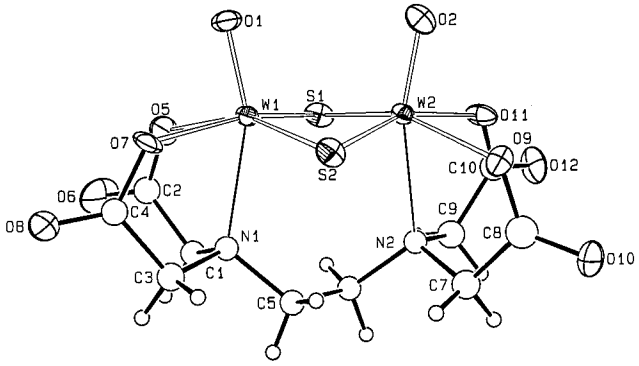

Figure 10. ORTEP representation of $[W_2O_2S_2(EDTA)]^{2-}$ anion, with atom labeling scheme. Selected bond distances (A) and angles (deg) (or their ranges): W1−W2 2.784(1), W1−S1 2.302(3), W1−S2 2.311(3), W2−S1 2.323(3), W2−S2 2.319(3), W1−O1 1.729(7), W2−O2 1.708(7), W1−N1 2.407(8), W2−N2 2.458(8), W−Oc 2.083−2.150, W−S−W 73.93−74.02, S−W−S 103.32−104.26, S−W−O1,2 103.6−105.6, S−W−N 80.95−91.69, N−W−O1,2 158.7−162.1.

anion and includes selected bond distances and angles. The overall structure is similar to that of the $[W_2O_4(EDTA)]^{2-}$ and $[W_2O_3S(EDTA)]^{2-}$ anions[129,130] and is almost identical to the structure of $NaNH_4[W_2O_2S_2(EDTA)]$ that first appeared in 1993.[131] Two tungsten atoms and two bridging sulfur atoms form a rhombohedron, and the two terminal oxo groups on each tungsten atom are in the cis configuration due to the constraints imposed by the EDTA ligand. The short W−W distance (2.784 Å) is clearly indicative of a W−W single bond.

2. Trinuclear Tungsten Cluster Compounds

$[W_3S_4(TTHA)]^{2-}$ anion was isolated from a reaction of TTHA and the corresponding nonaqua ion $[W_3S_4(H_2O)_9]^{4+}$ in refluxed DMF.[132] This reaction is unique in that the in situ degradation of DMF provides both the base for the deprotonation of

the TTHA ligand and also the counterion (NH_2Me^{2+}) for the cluster complex. The aqua ion $[W_3S_4(H_2O)_9]^{4+}$ was obtained on a 20 g scale through a modified literature procedure.[126,127] Cation metathesis through multiple ion exchange columns produced $H_2[W_3S_4(TTHA)]$. Neutralization with NaOH and NMG produced $Na_2[W_3S_4(TTHA)]$ and $(NMG)_2[W_3S_4(TTHA)]$ complexes.

$Na_2[W_3S_4(TTHA)]$ and $(NMG)_2[W_3S_4(TTHA)]$ are purple solids with aqueous solubilities of 0.17 and 0.5 M, respectively. The likely structure of the $[W_3S_4(TTHA)]^{2-}$ anion is shown in Figure 11, wherein

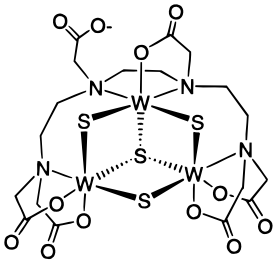

Figure 11. Schematic drawing of $[W_3S_4(TTHA)]^{2-}$ anion.

the cluster core of this compound, comprising three tungsten atoms and four sulfur atoms, is completely encompassed by a single TTHA ligand, as if the core were a single metal ion, to form a unique 1:1 cluster ligand complex.

3. Hexanuclear Tungsten Cluster Compound

A complex with two $[W_3S_4]$ cluster core units resulted from the reaction of EGTA and the nonaqua ion $[W_3S_4(H_2O)_9]^{4+}$ in refluxed DMF.[133] Isolation and cation exchange procedures analogous to the preparation of the $[W_3S_4(TTHA)]^{2-}$ complexes produced the corresponding $Na_4[(W_3S_4)_2(EGTA)_3]$ and $(NMG)_4[(W_3S_4)_2(EGTA)_3]$ complexes. They were both isolated as purple solids with aqueous solubilities of 0.04 and 0.072 M.

The crystal structure of $Na_4[(W_3S_4)_2(EGTA)_3]\cdot 29H_2O$ was determined by X-ray crystallography. A perspective view of the $[(W_3S_4)_2(EGTA)_3]^{4-}$ anion is shown in Figure 12. This is the first characterized

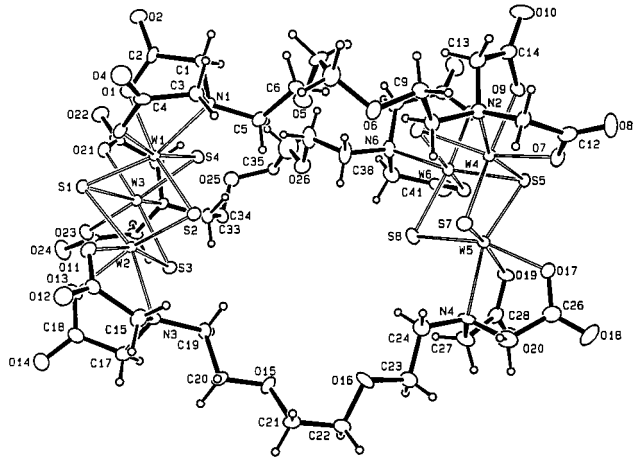

Figure 12. Perspective view of $[(W_3S_4)_2(EGTA)_3]^{2-}$ anion. (Reproduced with permission from ref 133. Copyright 1997 Elsevier Science.)

example of two W_3Q_4 (Q = O, S, Se) cluster units complexed by three linking polyaminopolycarboxylate ligands to form a discrete dimeric complex.

4. Other High Nuclearity Tungsten Compounds

From a technical standpoint tungsten heteropolyanions are not considered to be metal clusters. However, they contain multiple tungsten atoms in one molecule and can provide a high degree of X-ray attenuation. For comparative evaluation, a few well-known anions including $[PW_{12}O_{40}]^{3-}$, $[P_2W_{18}O_{62}]^{6-}$ and $[P_5W_{30}O_{110}]^{15-}$ were prepared according to literature methods.[134,135] Sodium salts were obtained, through ion exchange procedures, as white or off-white solids with various aqueous solubilities.

5. Safety and Efficacy Studies

The in vivo toxicities of several tungsten cluster compounds were examined in mice, and representative LD_{50} values are listed in Table 5. For some

Table 5. Solubility and Toxicity of Tungsten Cluster Complexes

	molecular solubility (M)	tungsten atom solubility (M)	LD_{50} (mmol/kg)
$Na_2[W_2O_4(EDTA)]$	0.5	1.0	10
$Na_2[W_2O_2S_2(EDTA)]$	0.075	0.15	~2.5 (MLD)
$(NMG)_2[W_2O_2S_2(EDTA)]$	0.3	0.6	~5 (MLD)
$Na_2[W_3S_4O(TTHA)]$	0.17	0.51	6.5
$(NMG)_2[W_3S_4O(TTHA)]$	0.49	1.47	7.2
$Na_4[(W_3S_4)_2(EGTA)_3]$	0.04	0.24	
$(NMG)_4[(W_3S_4)_2(EDTA)_3]$	0.072	0.43	4 (MLD)
$Na_2P_2W_{18}O_{64}$			$\ll$1 (MLD)

compounds, due to sample size limitations, only minimum lethal dosages (MLD, the largest administered dose survived by any of the test animals) could be determined. While the predictive power of this measurement is limited, it is likely that MLD is close to (but typically somewhat greater than) the actual LD_{50}. The toxicities were similar to those of the lanthanide DTPA complexes, particularly when compared on a molar metal ion basis, but the clusters were more toxic than the nonionic iodinated X-ray contrast agents.

There is a growing interest in evaluating polyoxometalates (tungsten heteropolyanions included) to treat cancer and viral diseases.[136] The IC_{50} value (effective concentration for 50% inhibition of cell growth in vitro) of the tungsten heteropolyanion is generally in the 0.1 mM range. This high toxicity probably arises from their high negative charge, by extrapolation with their use as precipitants for proteins.[137] An in vivo study in mice confirmed that all three tungsten heterpolyanions tested in CT were extremely toxic (MLD's less than 1 mmol/kg).[138]

A series of six representative tungsten cluster compounds, $Na_2[W_2O_4(EDTA)]$ (W2), $Na_2[W_3S_4(TTHA)]$ (W3), $Na_4[(W_3S_4)_2(EGTA)_3]$ (W6), $Na_3PW_{12}O_{40}$ (W12), α-$Na_6P_2W_{18}O_{62}$ (W18) and $Na_{15}P_5W_{30}O_{110}$ (W30), varying in tungsten nuclearity from 2 to 30 were evaluated in a CT phantom study using iohexol (I3) as a comparator. Five different concentrations of each compound were placed in a Siemens Somatom DRG CT scanner with Al and Cu filters operating at 125 kVp. Figure 13 plots CT numbers against the molar concentration for each compound tested. Linearity for

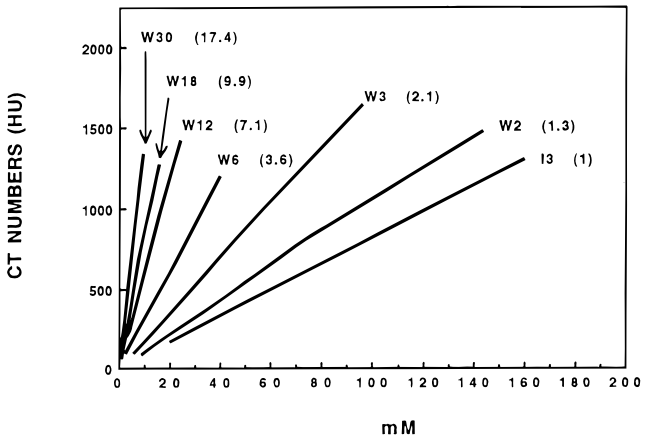

Figure 13. CT phantom study describing contrast enhancement in relation to the concentration of tungsten cluster complexes and iohexol at 125 kVp.

all compounds was good, and the slope for each series (plotting radiodensity versus molecular concentration) was proportional to the X-ray attenuation of the compound (the ratio of the slopes of each of the tungsten compounds and the iodine compound were the same as the ratio of the X-ray attenuations of the two materials). Hence, the ratio of the W3 compound and the I3 compound slopes was about 2:1, indicating that the X-ray attenuation produced by the three tungsten atoms in W3 was double that provided by the three iodine atoms in iohexol at 125 kVp.

An in vivo CT study compared $Na_2[W_3S_4(TTHA)]$ with iohexol in rats. Four regions of interest were continuously monitored after *iv* administration of each contrast agent. In all regions and time points, the enhancement produced by the tungsten cluster complex was about double that produced by iohexol, confirming the findings of the CT phantom study. The study also suggested that $Na_2[W_3S_4(TTHA)]$ and iohexol probably have similar pharmacokinetics profiles.[138]

The tremendous potential of tungsten cluster complexes as X-ray contrast agents was further demonstrated in a magnification angiography experiment in sedated rats. Angiograms of rat paw and forearm vasculature from sequential injections of 0.4 mL of iohexol 350 mg of I/mL (0.92 M) and an equal volume of $Na_6P_2W_{18}O_{62}$ (0.5 M) into the axillary artery. Initially, iohexol was injected to produce the angiogram presented in Figure 14b. Ten minutes later, $Na_6P_2W_{18}O_{62}$ was injected at the same speed to produce the second angiogram (Figure 14c). Figure 14a is an unenhanced X-ray of the region, demonstrating that the inherent contrast is limited to discriminating between bones and soft tissues. The tungsten compound produced a dramatic improvement in image quality. Blood vessels not visible with iohexol were visualized. Fine details of endothelial surfaces and of the lumen of the larger vessel were better seen on the tungsten angiogram. The utility of tungsten compounds as X-ray angiographic contrast agents is even better appreciated when one realizes that the largest blood vessels visualized in this study had a diameter of less than 1 mm and the images were taken at 75 kVp, i.e. a low-energy X-ray beam that has a bias toward iodinated agents.

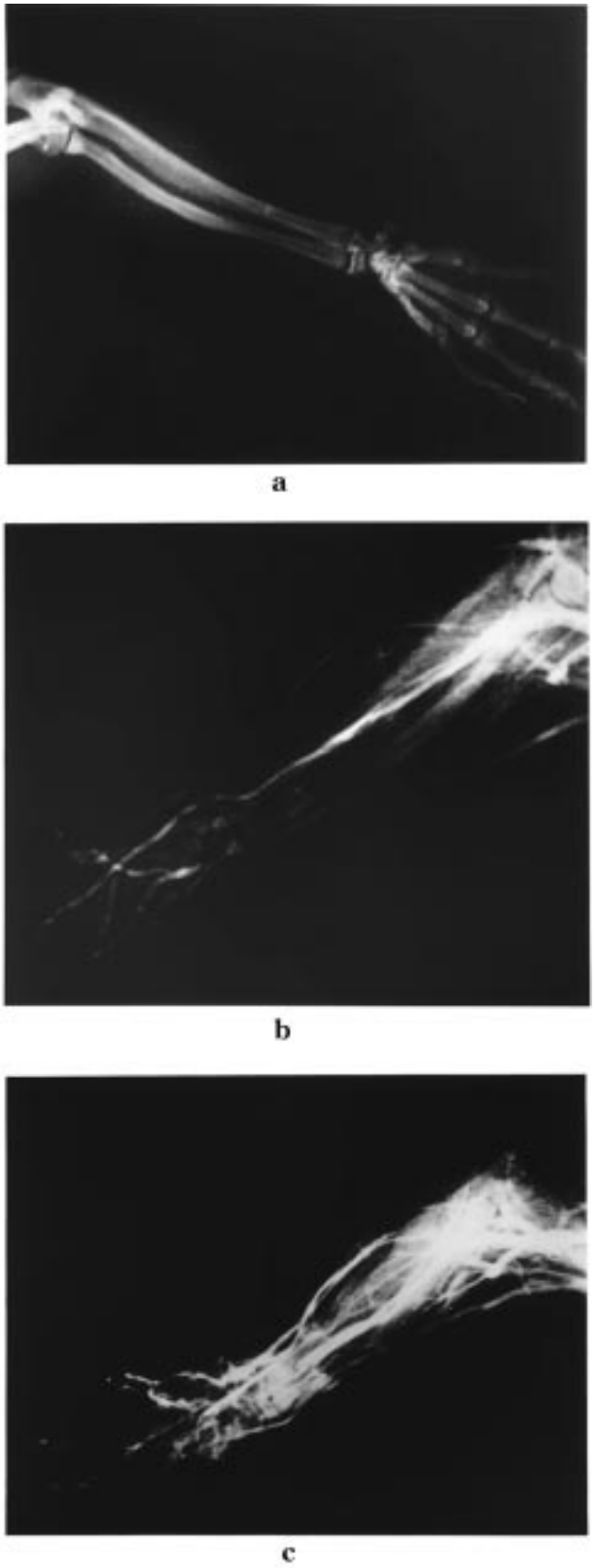

Figure 14. X-ray magnification images of a rat's forearm and paw (70 kVp). (A) No contrast enhancement. (B) After intraarterial injection of iohexol (0.4 mL; 0.92 and 2.8 M iodine). (C) After intraarterial injection of $Na_6[P_2W_{18}O_{62}]$ (0.4 mL; 0.5 and 9 M tungsten).

B. Other Tungsten Clusters

In addition to the cuboidal W_3Q_4 (Q = O, S) clusters tested as contrast agents, other types of multinuclear clusters with three or more tungsten atoms have been evaluated. Trinuclear clusters with monocapped and bicapped μ_3-oxygen bridges such as $[W_3(\mu_3\text{-}O)(\mu\text{-}CH_3CO_2)_6(H_2O)_3]^{2+}$ and $[W_3(\mu_3\text{-}O)_2(\mu\text{-}CH_3CO_2)_6(H_2O)_3]^{2+}$ are particularly interesting.[139−141] It is possible that the existing bridging carboxylate groups could be replaced by carboxylate groups containing hydroxyl groups to make the cluster complexes simultaneously both water-soluble and stable. Their X-ray attenuation ability should be similar to that of the W_3Q_4 clusters.

Hexanuclear tungsten clusters such as W_6X_8 (X = Cl, Br) are also attractive candidates for development as X-ray contrast agents.[142−146] A facile synthesis of a W_6Cl_8 cluster was reported recently.[147] Stable W_6I_8 clusters could also be particularly interesting structural templates:[148,149] one molecule of this cluster should produce aggregate X-ray attenuation equivalent to 20 iodine atoms and operate optimally over a wide kVp range, since as each tungsten atom is about twice as effective as each iodine atom. A series of complexes containing a hexanuclear tungsten cluster unit $[W_6X_8(CF_3SO_3)_6]^{2-}$ were prepared as possible entries into the chelate chemistry of this cluster system.[148,150] It should be possible to replace the labile triflate ligands with other ligands to impart water solubility and stability to these cluster complexes. However, successful replacement of trifluoromethanesulfonate with functional carboxylate-containing ligands has so far remained elusive.

The $[W_6S_8L_6]$ (L = PEt_3, Py) clusters are another interesting class of potential candidates.[151,152] However, to be useful as X-ray contrast agents, the phosphine or pyridine ligands which currently stabilize these cluster complexes will need to be replaced or modified to provide water solubility and cluster stability.

C. Other Heavy Metal Clusters

Molecular hexanuclear halide clusters of tantalum are also known.[153] The $[Ta_6Cl_{12}]^{4+}$ cluster with substitutionally labile triflate terminal ligands was reported recently,[154] and its metathesis with $(\mu\text{-}NC)\text{-}Mn(CO)_2Cp$ ligands was demonstrated. With the right ligands, the complexes of this cluster could be made water-soluble and stable. This octahedral hexanuclear metal cluster unit can also be found in interstitially stablized clusters (M = Hf, La, Pr, Le, Er, Gd, and Lu):[155,156] unfortunately, these clusters are all presently only found in the solid state. The exploration of their potential as X-ray contrast agents awaits further development of their solution chemistries.

One recent advance in the solution chemistry of hexanuclear rhenium chalcogenide clusters has produced interesting new metal cluster candidates with potential utility as X-ray contrast agents.[157] Cluster excision[158] and dimensional reduction[159] techniques extracted octahedral Re_6Q_8 (Q = S, Se) cluster units from these solid-state clusters into solution. With the help of a silver iodide salt, the terminal halides of these clusters could be replaced by phosphine and solvent ligands.[160,161] A fully solvated molecular cluster, $[Re_6Se_8(MeCN)_6]^{2+}$, was obtained which could undergo further substitution, aimed at producing soluble stable cluster complexes. In addition, such single hexanuclear cluster compounds might be condensed into molecular clusters with multiple Re_6Se_8 units using thermolysis techniques.[162] The rhomb-linked molecular dicluster $Re_{12}Se_{16}$ and tetracluster $Re_{24}Se_{32}$ were produced from partially solvated and ligated hexanuclear clusters.

VI. Organobismuth Compounds as X-ray Contrast Agents

The known chemistry of organobismuth compounds primarily involves the Bi(III) and Bi(V) oxidation states, with Bi(III) compounds generally being the more stable. Extensive reviews on the preparation, reaction chemistry, and physical properties of organobismuth compounds are readily available.[163] In addition to the advantages inherent to all the heavy metal compounds so far described, organobismuth compounds have two additional distinct advantages which suggest their consideration as X-ray contrast agents. (1) The covalent bond between bismuth and aromatic carbon atoms is relatively strong (194 kJ/mol), and many triarylbismuth compounds are known to be very stable. This is similar to the strong covalent bond between iodine and carbon atoms on the aromatic ring (bond dissociation energy 266 kJ/mol) of the tri-iodobenzene system and (2) Organobismuth compounds are usually nonionic unlike metal complexes and metal cluster complexes which are usually formulated as salts.

A series of triaryl bismuth compounds was synthesized (Figure 15) where the substituents X_1, X_2

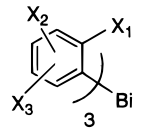

Figure 15. Schematic drawing of representative triarylbismuth compounds.

and X_3 were hydroxyl groups designed to impart aqueous solubility to these compounds. One bismuth compound in the series (where $X_1 = SO_2N(CH_2CH_2OH)_2$, $X_2 = 4\text{-}SO_2N(CH_2CH_2OH)_2$ and X_3 = H) could be formulated as a 55% w/v water solution. An in vitro X-ray CT phantom study (80 kVp) compared its X-ray attenuation with that of an iodinated agent formulated at 15% w/v (iopamidol, a nonionic monomer). The measured CT number for the bismuth compound was 2764 HU comparable to the CT number 3085 HU for iopamidol.

A 28.5% w/v saline solution of the same bismuth compound was administered to mice to study its toxicity. At a dose of 11.4 g/kg, all mice exhibited a spontaneous decrease in motion which returned to normal within 2 h. There were no other significant symptoms over the following 7 days and no mice died.

The partition coefficient of this bismuth compound between 1-octanol:water was determined to be $P = 0.00199$ which is comparable to that of iopamidol ($P = 0.0025$). This class of water-soluble triaryl bismuth compounds may have prospects as intravascular X-ray contrast agents.

Triaryl bismuth compounds have also been considered in the preparation of radiopaque resins.[165] Triphenylbismuth was used as an additive and *p*-styryldi(*p*-tolyl)bismuth was used as a monomer for the copolymerization with acrylates or other monomers.[166] Such light transparent materials can provide radiopacities exceeding that of aluminum and are proportional to the amount of bismuth incorporated in the resin. The cytotoxicity (cell killing ability) of triphenylbismuth and its polymeric resins has been assessed[167] and fall at the lower end of the range exhibited by representatives of comparable biomaterials.[167] The use of these radiopaque resins as components of polymer-based medical devices such as sutures, catheters, implants, and dental materials has been suggested.

VII. Concluding Remarks

Spanning more than 50 years, progress toward the development of new metal-based drug candidates as X-ray contrast agents has been quite remarkable given the complexity of the chemical and biological challenges involved together with the very high safety and efficacy benchmarks presented by the existing classes of iodinated materials which are now in routine use. The cluster chemistry developed over the past 8 years alone, described in section V of this article, suggests the very real prospect this chemistry offers to the genesis of a class of inexpensive metal-based X-ray contrast agents originating from new technological and chemical approaches. For the first time, such agents will be able to be "tuned" (for example, tungsten in a contrast agent to the tungsten X-ray tubes) to provide coherence at a specific X-ray tube voltage in order to provide a level of performance far beyond that of the conventional X-ray agents used today.

For a heavy metal-based X-ray contrast agent to be competitive with water-soluble iodinated agents for general intravascular use, it should possess at least the following attributes: (1) it must have a high degree of water solubility (at least 2 M per metal atom), (2) it must be stable at physiological pH, at room temperature and under normal storage conditions, (3) its pharmacokinetic profile should be similar to that of the established iodinated agents, (4) it must be completely excreted once it has served its diagnostic purpose, (5) it needs to be extremely safe, causing minimal patient discomfort and no acute or delayed reactions. The safety assessment must also consider potential immunogenicity, carcinogenicity, mutagenicity and teratogenicity factors, and (6) It must be readily and easily injectable, necessitating an osmolality that does not alter the osmotic balance of the plasma and a viscosity that allows a concentrated solution of the agent to flow readily on injection.

It is unlikely that any simple heavy metal salts or metal particulates will be useful as intravascular X-ray contrast agents simply due to their likely acute and long-term toxicities and the inability of the human body to completely excrete them. Heavy metal complexes, particularly DyEOB-DTPA and GdDO3A-butrol, hold some technical potential to be developed as the first metal-based X-ray agents (outside of barium) to be indicated for human use. They may find application in niche indications, such as for intravascular use in patients that are contraindicated to iodinated agents or as liver-specific CT agents. However, general intravascular use of a heavy metal complex is likely to be limited by safety concerns and dosage requirements. Furthermore, their relatively low aqueous solubility will also restrict their utility and limit their consideration as general extracellular X-ray contrast agents.

Heavy metal cluster complexes have the potential to bridge the gap between metal salts or particulates (more heavy metal ions per unit volume but poor safety profiles) and metal complexes (sufficiently safe but poor efficacy since the metal ion concentration per unit volume is low). Molecular metal clusters by definition contain two or more metal ions per molecule. One hexanuclear heavy metal cluster is capable of producing a degree of X-ray contrast enhancement equal to that produced by four monomeric triiodobenzene-based molecules. This high contrast enhancement per unit volume enables a heavy metal cluster complex to uniquely produce a level of contrast enhancement that just cannot be obtained with the current generation of iodinated agents.

Finally, healthcare economics will play a significant role in determining whether a metal-based agent can ever truly be a viable replacement for the current inexpensive iodinated agents. Unlike other pharmaceuticals or even contrast agents for MRI, the quantity of iodinated material administered in a single dose is considerable. A typical dose of iodinated contrast media contains between 20 and 70 g of iodine formulated as a 200−350 mg of I/mL aqueous solution. Even though the dose for a hypothetical replacement heavy metal-based contrast agent might be lower, multigram quantities of a heavy metal would still be required and may be quite expensive. Table 6 lists the abundance of selected naturally occurring elements with $Z \geq 50$ in the Earth's crust and their cost per gram (abundance is inversely proportional to cost as one might expect). However, there are a few exceptions: bismuth (with a very low abundance) is relatively inexpensive, while on the other hand (despite their high abundance) the costs for europium, thullium, and lutetium are prohibitively high. It is possible that if the demand for increased volumes of a particular heavy metal picks up, new production processes might be developed which could significantly lower prices.

From the list of possible heavy metals, we may exclude those metals that are radioactive (Th, U), those that are highly toxic (real or perceived) in any form (Hg, Pb, Tl, Cd, Ag) or those that are unduly expensive (Pt, Ir, Os, Au, Pd) from consideration. Furthermore, those elements close to iodine (In−Ba)

Table 6. Nature Abundance and Cost of Selected Heavy Metals

atomic number	element	abundance in the earth's crust (ppm)[a]	cost ($/g)[b]
50	Sn	2.1	0.068
53	I	0.46	0.113
55	Cs	2.5	5.73
56	Ba	390	0.488
57	La	35	1.34
58	Ce	66	0.772
59	Pr	9.1	2.02
60	Nd	40	0.364
62	Sm	7.0	1.51
63	Eu	2.1	40.2
64	Gd	6.1	2.76
65	Tb	1.2	10.36
66	Dy	4.5	1.59
67	Ho	1.3	8.08
68	Er	3.5	2.7
69	Tm	0.5	39.2
70	Yb	3.1	5.76
71	Lu	0.8	74
72	Hf	2.8	0.96
73	Ta	1.7	1.19
74	W	1.2	0.1045
75	Re	0.0007	8.12
76	Os	0.005	59.12
77	Ir	0.001	44.6
78	Pt	0.01	52.24
79	Au	0.004	13.6
80	Hg	0.08	0.006
81	Tl	0.7	1.246
82	Pb	13	0.01
83	Bi	0.008	0.07
90	Th	8.1	24.7
92	U	2.3	4.92

[a] Emsley, J. *The Elements*; Oxford University Press: New York, 1989. [b] Lowest price available from the Alfa catalog, 1997−98.

do not offer any advantages over iodine in terms of their ability to utilize high-energy X-ray photons (thus lowering the radiation exposure to patients) and can also be eliminated. This leaves only the lanthanide metals and Hf, Ta, W, Re, and Bi as potential candidates.

The chelation chemistry of the lanthanide metal ions has been greatly expanded during the past two decades and permits the design of metal complexes with improved water solubility and stability. The addition of functional groups may even be used to make these complexes somewhat tissue-specific. However, these advances not withstanding, it is difficult to envision that a heavy metal complex X-ray contrast agent based around a single metal atom will realistically be fully developed as a general extracellular X-ray contrast agent.

The cluster chemistries of Ta, W, and Re are extensive and well developed. The complexation of cuboidal trinuclear tungsten clusters with common chelating agents has been successfully demonstrated and such complexation shown to greatly improve the stability of the cluster core, permitting commercial-scale quantities of these complexes to be isolated. For example, W_3S_4 aqua ion is somewhat air sensitive and only stable in strong acidic conditions (1 M HCl or stronger). Yet the two complexes $[W_3S_4(TTHA)]^{2-}$ and $[(W_3S_4)_2(EGTA)_3]^{4-}$ are stable in air and in aqueous solutions (pH 2−10) almost indefinitely. Progress in the design and synthesis of new chelating agents may permit the isolation of a metal cluster complex that is highly water soluble and biologically tolerable. It is certainly possible that a viable intravascular agent for general use might emerge from the metal cluster complex chemistry of Ta, W, or Re.

Neither the coordination chemistry nor the cluster chemistry of bismuth is very well developed. However, organometallic compounds of Bi(III) with aryl groups are often stable. Derivitization of the aryl groups with hydroxy groups has produced Bi(III) aryl compounds that are both water soluble and stable. To compete with iodinated agents, it may be necessary for a bismuth molecule to contain two or more bismuth atoms on one benzene ring, and this poses a significant synthetic challenge.[168] Due to its high degree of X-ray contrast and a high K edge suitable to very high X-ray photon energies, an X-ray contrast agent based on an organobismuth compound could be a competitor to the iodinated agents.

The extremely safe and efficacious iodinated X-ray contrast agents in routine clinical use today set a very high standard to overcome for a first-generation heavy metal-based X-ray contrast agent. The iodine-containing agents have moved through several product iterations from ionic to nonionic, monomers to dimers, high to low osmolality and viscosity formulations and in each case derived additional benefits in either improved safety or efficacy. These materials have now been injected into tens of millions of patients with overall minimal adverse effects and performed admirably well. The need to produce hundreds of tons of these agents each year has also resulted in massive economics of scale in their production, formulation, and distribution.

The challenge to move to an entirely new technology platform and successfully develop an adequate first-generation metal-based compound which could compete with the current generation of iodinated materials is immense and in our minds presently remains unsolved. However, tantalizing clues (many described in this review) have been elicited (particularly over the past 10 years) as to which research directions might lead to viable drug candidates. We believe sufficient proof-of-principle research has been done to establish the possibility inherent in this concept and hope chemists at large will take up the challenge to develop ever more stable and water-soluble chelate cluster complexes which could provide new classes of X-ray contrast agents.

VIII. Acknowledgment

We thank our co-workers Brent Segal, Tony Sanderson, Shannon Downey, Sook-hui Kim, Jere Fellman, Dirk Bergstrom, Shaun Crofts, Bill Newcome, Bill Nelson, and Naidong Ye for their contribution to the work which was carried out at Nycomed Salutar Inc. under the supervision of Micheal Droege. We also thank Torsten Almén, Arne Berg, Jo Klaveness, Jan-Ove Christoffersson and Richard H. Holm for their advice and support. Finally, we thank Eric Hohenschuh and Geraldine Cooney for their assistance in the preparation of this manuscript.

IX. References

(1) Roentgen, W. C. On a New Kind of Rays. *Sitzungsber. Phys. Med. Ges. Wurzburg* **1895**, *137*, S132−1141.
(2) Eisenberg, R. L. *Radiology, An Illustrated History*; Morsby-Year Book: St. Louis, 1992.
(3) Sunshine, J. H.; Mabry, M. R.; Bansal, S. *Am. J. Roentgenol.* **1991**, *157*, 609.
(4) Jeans, J.; Vermeeren, P. *Eur. J. Nucl. Med.* **1998**, *25*, 1469.
(5) Editorial staff, *Diagnostic Imaging Industry Report: Update 1996*; Miller Freeman: San Francisco, 1996.
(6) POV Reports *The Diagnostic Imaging Marketplace In the U.S.*; POV Inc.: Cedar Grove, NJ, 1998.
(7) Bachem, C.; Gunther, H. *Z. Fhr Rontgenkunde* **1910**, *12*, 369.
(8) Theoni, R. F.; Margulis, A. F. *Radiology* **1988**, *167*, 1.
(9) Skucas, J. *Radiographic Contrast Agents*, 2nd ed.; Aspen Publishers: Rockville, MD, 1989.
(10) Grainger, R. G. *Br. J. Radiol.* **1982**, *55*, 1.
(11) Sovak, M. *Invest. Radiol.* **1994**, *29*, S1.
(12) Palmisano, S. M. *Radiology* **1997**, *203*, 309.
(13) Osborne, E. D.; Sutherland, C. G.; Scholl, A. J., Jr.; Rowntree, L. G. *J. Am. Med. Assoc.* **1923**, *80*, 368.
(14) (a) Swick, M. *Klin. Wochenschr.* **1929**, *8*, 2087. (b) Swick, M. *Surg. Clin. N. Am.* **1978**, *58*, 977.
(15) Binz, A. J. *Urology* **1931**, *25*, 297.
(16) (a) Katzberg, R. W. *Radiology* **1997**, *204*, 297. (b) Krause, W.; Niehues, D. *Invest. Radiol.* **1996**, *31*, 30. (c) Visipaque (Iodixanol) package insert. Nycomed-Amersham Imaging. 1999.
(17) (a) Katayama, H.; Yamaguchi, K.; Kozuka, T.; Takashima T.; Seez, P.; Matsuura, K. *Radiology* **1990**, *175*, 621. (b) McClennan, B. L. *Invest. Radiol.* **1994**, *29*, S46.
(18) Almén, T. J. *Theor. Biol.* **1969**, *24*, 216.
(19) Almén, T. *Invest. Radiol.* **1994**, *29*, S37.
(20) Seigel, E. L. *Acad. Radiol.* **1996**, *3*, S528.
(21) For a thorough discussion on the medical physics of X-ray contrast, see: (a) Curry, T. S., III; Downdey, J. E.; Murry, R. C., Jr. *Christensen's Physics of Diagnostic Radiology*, 4th ed.; Lea & Febiger: Philadelphia, 1990. (b) Hendee, W. R.; Ritenour, R. *Medical Imaging Physics*, 3rd ed.; Mosby-Year Book: St. Louis, 1992.
(22) Lumbroso, P.; Dick, C. E. *Med. Phys.* **1987**, *14*, 752.
(23) (a) Fryar, J.; O'Hare, N. J.; Dowsett, D. J. *Proced. SPIE Int. Soc. Op. Eng.* **1990**, *1231*, 246. (b) O'Hare, N. *J. Phys. Med. Biol.* **1992**, *37*, 1519.
(24) Ruth, C.; Joseph, P. M. *Med. Phys.* **1995**, *22*, 1977.
(25) Sandborg, M.; Christoffersson, J.-O.; Carlsson, G. A.; Almen, T.; Dance, D. R. *Phys. Med. Biol.* **1995**, *40*, 1209.
(26) (a) Seltzer, S. E.; Davis, M. A.; Judy, P. F.; Havron, A. *Invest. Radiol.* **1979**, *14*. 400. (b) Seltzer, S. E. *Int. Congr. Ser. Excerpta Medica* (EXMDA4) **1981**, *561*, 76.
(27) For a more extensive description of X-ray diagnostic imaging procedures, see: (a) Eisenberg, R. L. *Diagnostic Imaging in Internal Medicine*; McGraw-Hill: New York, 1985. (b) *A Global Textbook of Radiology*; Pettersson, H., Ed.; The NICER Institute: Oslo, 1995.
(28) Internal marketing reports, Nycomed Amersham Imaging.
(29) Voelcker, F.; von Lichtenberg, A. *Muench. Med. Wochenschr.* **1906**, *53*, 105.
(30) Uhle, A. A.; Pfahler, G. E.; MacKinney, W. H.; Miller, A. G. *Ann. Surg.* **1910**, *51*, 546.
(31) (a) Seltzer, S. E.; Adams, D. F.; Davis, M. A.; Hessel, S. J.; Hurlburt, A.; Havron, A.; Hollenberg, N. K. *Invest. Radiol.* **1979**, *14*. 356. (b) Seltzer, S. E.; Adams, D. F.; Davis, M. A.; Hessel, S. J.; Havron, A.; Judy, P. F.; Pashins-Hurlburt, A. J.; Hollenberg, N. K. *J. Comput. Assist. Tomogr.* **1981**, *5*. 370. (c) Havron, A.; Davis, M. A.; Seltzer, S. E.; Paskins-Hurlburt, A. J.; Hessel, S. J. *J. Comput. Assist. Tomogr.* **1980**, *4*, 642.
(32) Rumpel, T. *Muenchen Med. Wschr.* **1897**, *44*, 420.
(33) Cannon, W. B. *Am. J. Physiol.* **1898**, *1*, 359.
(34) Kassabian, M. K. *Roentgen Rays and Electrotherapeutics*; JB Lippincott: Philadelphia, 1907.
(35) (a) Springer, K. *Prager Med. Wochenschr.* **1906**, *31*, 162. (b) Jackson, C. *Am. J. Roentgen* **1918**, *5*, 454.
(36) Wuff, P. *Fortschr. Roentgenstr.* **1904**, *8*, 193.
(37) Saito, K.; Oosato, F.; Ochiai, Y.; Tanaka, T.; Wachi, H.; Morokuma, T. Japanese Patent Application 95−43527, 1995; *Chem. Abstr.* **1995**, *125*, 257292.
(38) Abe, I. Japanese Patent Application 90−104206, 1990; *Chem. Abstr.* **1990**, *116*, 262525.
(39) (a) Shapiro, R. *Acta Radiol.* **1956**, *46*, 635. (b) Shapiro, R.; Papa, O. *Ann. N.Y. Acad. Sci.* **1959**, *78*, 756.
(40) Burns, J. E. *Bull. Johns Hopkins Hosp.* **1916**, *27*, 157.
(41) Waters, C. A.; Bayne-Jones, S.; Rowntree, L. G. *Arch. Intern. Med.* **1917**, *19*, 538.
(42) (a) Moniz, E.; Pinto, A.; Lima, A. *Rev. Neurol.* **1931**, *32*, 646. (b) Moniz, E.; Pinto, A.; Lima, A. *Roentgenpraxis* **1932**, *4*, 90.
(43) Radt, P. *Med. Klin.* **1930**, *26*, 1889.
(44) (a) Dickson, W. H. *Can. Med. Assoc. J.* **1932**, *27*, 125. (b) Irwin, D. A. *Can. Med. Assoc. J.* **1932**, *27*, 130. (C) Macdonald, I. G. *Can. Med. Assoc. J.* **1932**, *27*, 136.
(45) Council on Pharmacy and Chemistry of the American Medical Association *J. Am. Med. Assoc.* **1932**, *99*, 2193.
(46) Abbatt, J. D. *Environ. Res.* **1979**, *18*, 6.
(47) Loman, J.; Myerson, A. *Am. J. Roentgen* **1936**, *35*, 188.
(48) Yater, W. M.; Otell, L. S. *Am. J. Roentgen* **1933**, *29*, 172.
(49) (a) Thomas, S. F.; Henry, G. W.; Kaplan, H. S. *Radiology* **1951**, 57, 669. (b) Thomas, S. F. *Radiology* **1962**, *78*, 435.
(50) Janower, M. L.; Miettinen, O. S.; Flynn, M. J. *Radiology* **1972**, *103*, 13.
(51) Ono, N.; Hirai, K.; Jiyuin, H.; Itano, S.; Noguchi, H.; Sakata, K.; Aoki, Y.; Aritaka, T.; Abe, H.; Tanikawa, K. *Clin. Imag.* **1995**, *19*, 229.
(52) Kitamura, K.; Imazawa, Y.; Morimoto, T.; Sato, K.; Higuchi, H.; Imai, K.; Watari, K. *J. Radioanal. Nucl. Chem.* **1997**, *217*, 175.
(53) Humphreys, J. A. H.; Priest, N. D.; Ishikawa, Y. *Health Phys.* **1998**, *74*, 442.
(54) Andersson, M.; Juel, K.; Strom, H. H. *J. Clin. Epidemiol.* **1993**, *46*, 637.
(55) (a) Fischer, H. W. *Radiology* **1957**, *68*, 488. (b) Fischer, H. W. *Am. J. Roentgen* **1957**, *77*, 64.
(56) Fischer, H. W.; Zimmerman, G. R. *Arch. Pathol.* **1969**, *88*, 259.
(57) Gellermann, C.; Wolter, H.; Storch, W. *Mater. Res. Soc. Symp. Proc.* **1998**, *520*, 185.
(58) Shapiro, R. *Radiology* **1955**, *65*, 429.
(59) Hunter, S. W.; Miree, J.; Bloch, H. *Surgery* **1949**, *26*, 682.
(60) McClinton, L. T.; Schubert, J. *J. Pharmacol. Exp. Ther.* **1948**, *94*, 1.
(61) Lerouge, S.; Huk, O.; Yahia, L. H.; Sedel, L. *J. Biomed. Mater. Res.* **1996**, *32*, 627.
(62) Nadel, J. A.; Wolfe, W. G.; Graf, P. D.; Youker, J. E.; Zamel, N.; Austin, J. H. M.; Hinchcliffe, W. A.; Greenspan, R. H.; Wright, R. R. *N. Engl. J. Med.* **1970**, *283*, 281. (b) Dilley, R. B.; Nadel, J. A. *Ann. Otol. Rhinol., & Laryngol.* **1970**, *79*, 945. (c) Hinchcliffe, W. A.; Zamel, N.; Fishman, N. H.; Dedo, H. H.; Greenspan, R. H.; Nadel, J. A. *Radiology* **1970**, *97*, 327.
(63) Stitik, F. P.; Proctor, D. F. *Ann. Otol. Rhinol. Laryngol.* **1973**, *82*, 838.
(64) House, A. J. S. In *Radiographic Contrast Agents*, 1st ed.; Skucas, J., Ed.; Aspen Publishers: Rockville, MD, 1977; p 411.
(65) Nadel, J. A.; Wolfe, W. G.; Graf, P. D. *Invest. Radiol.* **1968**, *3*, 229.
(66) Sargent, N.; Sherwin, R. *Am. J. Roentgen* **1971**, *113*, 660.
(67) Edmunds, L. H., Jr.; Graf, P. D.; Sagel, S. S.; Greenspan, R. H. *Invest. Radiol.* **1970**, *5*, 131.
(68) Friedman, P. J.; Tisi, G. M. *Radiology* **1972**, *104*, 523.
(69) Schelesinger, R. B.; Schweizer, R. D.; Chan, T. L.; Keegan, A. L.; Lippmann, M. *Invest. Radiol.* **1975**, *10*, 115.
(70) Gamsu, G.; Platzker, A.; Gregory, G.; Graf, P.; Nadel, J. A. *Radiology* **1973**, *107*, 151.
(71) Gamsu, G.; Weintraub, R. M.; Nadel, J. A. *Am. Rev. Respir. Dis.* **1973**, *107*, 214.
(72) Upham, T.; Graham, L. S.; Steckel, R. J.; Poe, N. *Am. J. Roentgen.* **1971**, *111*, 690.
(73) Bianco, A.; Gibb, F. R.; Kilpper, R. W.; Landman, S.; Morrow, P. E. *Radiology* **1974**, *112*, 549.
(74) Von Sailer, R.; Kissler, B.; Stauch, G.; Franken, T.; Huth, F. *Forstchr. Rontgenstr.* **1973**, *119*, 727.
(75) Dumont, A. E.; Martelli, A. *Lymphology* **1969**, *2*, 91.
(76) Nadel, J. A.; Dodds, W. J.; Goldberg, H.; Graf, P. D. *Invest. Radiol.* **1969**, *4*, 57.
(77) Goldberg, H.; Dodds, W. J.; Jenis, E. H. *Am. J. Roentgen* **1970**, *110*, 288.
(78) Rutkowiak, B. *Pol. Arch. Weter.* **1977**, *20*, 79.
(79) Dumont, A. E.; Acinapura, A.; Martelli, A. B.; Biris, L. *Invest. Radiol.* **1972**, *7*, 56.
(80) Casasco, A.; Herbreteau, D.; Houdart, E.; George, B.; Tran Ba Huy, P.; Deffresne, D.; Merland, J. J. *Am. J. Neuroradiol.* **1994**, *15*, 1233.
(81) Link, D. P.; Mourtada, F. A.; Jackson, J.; Blashka, K.; Samphilipo, M. A. *Invest. Radiol.* **1994**, *29*, 746.
(82) Clement, O.; Siauve, N.; Cuenod, C.-A.; Frija, G. *Top. Man. Reson. Imaging* **1998**, *9*, 167.
(83) Bessman, S. P.; Rubin, M.; Leikin, S. *Pediatrics* **1954**, *14*, 201.
(84) Lauffer, R. B. *Chem. Rev.* **1987**, *87*, 901.
(85) (a) Cacheris, W. P.; Quay, S. C.; Rocklage, S. M. *Magn. Reson. Imaging* **1990**, *8*, 467. (b) Rocklage, S. M.; Watson, A. D.; Carvlin, M. J. In *Magnetic Resonance Imaging*, 2nd ed.; Stark, D. D., Bradley, W. G., Eds.; Mosby-Year Book: St. Louis, 1992; p 372. (c) Hohenschun, E.; Watson, A. D. In *Magnetic Resonance Imaging of the Body*, 3rd ed.; Higgins, C. B., Hricak, H., Helms, C. A., Eds.; Lippincott-Raven: Philadelphia, 1997; p 1439.
(86) Kumar, K.; Chang, C. A.; Tweedle, M. F. *Inorg. Chem.* **1993**, *32*, 587.
(87) Toth, E.; Brucher, E.; Lazar, I.; Toth, I. *Inorg. Chem.* **1994**, *33*, 4070.

(88) Platzek, J.; Blaszkiewicz, P.; Gries, H.; Luger, P.; Michi, G.; Muller-Fahrnow, A.; Raduchel, B.; Sulzle, D. *Inorg. Chem.* **1997**, *36*, 6086.
(89) Janon, E. A. *Am. J. Roentgen* **1989**, *152*, 1348.
(90) Engelbrecht, V.; Koch, J. A.; Rassek, M.; Modder, U. *Fortschr. Rontgenstr.* **1996**, *165*, 24.
(91) Unger, E.; Gutierrez, F. *Invest. Radiol.* **1986**, *21*, 802.
(92) (a) Zwicker, C.; Langer, M.; Langer, R.; Keske, U. *Invest. Radiol.* **1991**, *26*, S162. (b) Zwicker, C.; Langer, M.; Urich, V.; Felix, R. *Fortschr. Rontgenstr.* **1993**, *158*, 255.
(93) Bush, W. H.; Swanson, D. P. *Am. J. Roentgen* **1991**, *157*, 1153. (b) Rudnick, M. R.; Goldfarb, S.; Wexler, L.; Ludbrook, P. A.; Murphy, M. J.; Halpern, E. F.; Hill, J. A.; Winniford, M.; Cohen, M. B.; VanFossen, D. B. *Kidney Int.* **1995**, *47*, 254.
(94) Bloem, J. L.; Wondergem, J. *Radiology* **1989**, *171*, 578.
(95) Gibson, R. J.; Meanock, C. I.; Torre, E. P. H.; Walker, T. M. *Clin. Radiol.* **1993**, *47*, 278.
(96) Quinn, A. D.; O'Hare, N. J.; Wallis, F. J.; Wilson, G. F. *J. Comput. Assist. Tomogr.* **1994**, *18*, 634.
(97) Kinno, Y.; Odagiri, K.; Andoh, K.; Itoh, Y.; Tarao, K. *Am. J. Roentgen* **1993**, *160*, 1293.
(98) Schild, H. H.; Weber, W.; Boeck, E.; Mildenberger, P.; Strunk, H.; Duber, Ch.; Grebe, P.; Schadmand-Fischer S.; Thelen, M. *Fortschr. Rontgenstr.* **1994**, *160*, 218.
(99) Matchett, W. J.; McFarland, D. R.; Russell, D. K.; Sailors, D. M.; Moursi, M. M. *Radiology* **1996**, *201*, 569.
(100) Kaufman, J. A.; Geller, S. C.; Waltman, A. C. *Radiology* **1996**, *198*, 579.
(101) (a) Vehmas, T.; Tervahartiala, P. *Acta Radiol.* **1996**, *37*, 804. (b) Vehmas, T.; Markkola, T. *Acta Radiol.* **1998**, *39*, 223.
(102) Weinmann, H. J.; Lanaido, M.; Mutzel, W. *Physiol. Chem. Phys. Med. NMR* **1984**, *16*, 167. (b) Olson, B.; Aulie, A.; Sveen, K.; Andrew, E. *Invest. Radiol.* **1983**, *18*, 177.
(103) VanWagoner M.; O'Toole, M.; Worah, D.; Leese, P. T.; Quay, S. C. *Invest. Radiol.* **1991**, *26*, 980.
(104) Fobbe, F.; Wacher, F.; Wagner, S. *Eur. Radiol.* **1996**, *6*, 224.
(105) Spinosa, D. J.; Matsumoto, A. H.; Angle, J. F.; Hagspiel, K. D.; McGraw, J. K.; Ayers, C. R. *Radiology* **1998**, *209(p)*, 490.
(106) Staks, T.; Schuhmann-Giampieri, G.; Frenzel, T.; Weinmann, H. J.; Lange, L.; Platzek, J. *Invest. Radiol.* **1994**, *29*, 709.
(107) (a) Schmitz, S. A.; Wagner, S.; Schuhmann-Giampieri, G.; Wolf, K. *Invest. Radiol.* **1995**, *30*, 644. (b) Schmitz, S. A.; Wagner, S.; Schuhmann-Giampieri, G.; Krause, W.; Wolf, K. *Radiology* **1996**, *201(p)*, 350.
(108) Dorey, J. H.; Aaron, J. O. *Radiology* **1993**, *189(p)*, 242.
(109) Gianturco, L. E.; Gale, D. R.; Feldman, L.; Cantelmo, N.; Gale, M. E. *Radiology* **1996**, *201(p)*, 314.
(110) McLachlan, S. J.; Eaton, S.; DeSimone, D. N. *Invest. Radiol.* **1991**, *27*, S12.
(111) (a) Balzer, T.; Hamm, B.; Staks, T.; Weinmann, H. J.; Muhler, A.; Taupitz, M.; Niendorf, H. P. In *New Developments in Contrast Agent research*; Rinck, P. A., Muller, R. N., Eds.; European Magnetic Resonance Forum: Berlin, 1995; p 129. (b) Hamm, B.; Staks, T.; Muhler, A.; Bollow, M.; Taupitz, M.; Frenzel, T.; Wolf, K. J.; Weinmann, H. J.; Lange, L. *Radiology* **1995**, *195*, 785. (c) Schumann-Giampieri, G.; Schitt-Willich, H.; Frensel, T. *J. Pharm. Sci.* **1993**, *82*, 799. (d) Schumann-Giampieri, G.; Schitt-Willich, H.; Press: W.; Negishi, C.; Weinmann, H. J.; Speck, U. *Radiology* **1992**, *183*, 59. (e) Schumann-Giampieri, G.; Mahler, M.; Röll, G.; Maibauer, R.; Schmitz, S. *J. Clin. Pharmacol.* **1997**, *37*, 587.
(112) Krause, W.; Schuhmann-Giampieri, G.; Bauer, M.; Press: W. F.; Muschick, P. *Invest. Radiol.* **1996**, *31*, 502.
(113) (a) Schmitz, S. A.; Wagner, S.; Schuhmann-Giampieri, G.; Krause, W.; Wolf, K. *Radiology* **1997**, *202*, 407. (b) Rupp, K.; Handreke, K.; Schuhmann-Giampieri, G.; Krause, W.; Hamm, B. K. *Radiology* **1997**, *205(p)*, 338. (c) Krause, W.; Handreke, K.; Rupp, K.; Schuhmann-Giampieri, G.; Muschick, P.; Hamm, B. K. Radiology **1997**, *205(p)*, 319. (d) Schuhmann-Giampieri, G.; Rupp, K.; Muschick, P.; Treher, M.; Krause, W. Acad. Radiol. **1998**, *5*, S90.
(114) Schmitz, S. A.; Haberle, J. H.; Balzer, T.; Shamsi, K.; Boese-Landgraf, J.; Wolf, K. J. *Radiology* **1997**, *202*, 399.
(115) Rubin, M.; Di Chiro, G. *Ann. N.Y. Acad. Sci.* **1959**, *78*, 764.
(116) Shapiro, R. *Am. J. Roentgen* **1956**, *76*, 161.
(117) Tjernberg, B. *Acta Radiol.* **1957**, *47*, 308.
(118) Sapeika, N. *Br. J. Med.* **1955**, *2*, 167.
(119) Foreman, H. *Br. J. Med.* **1955**, *2*, 678.
(120) Nalbandian, R. M.; Rice, W. T.; Nickel, W. O. *Ann. N.Y. Acad. Sci.* **1959**, *78*, 779.
(121) (a) Fijibayashi, Y.; Sakakibara, H.; Fukumoto, S.; Yokoyama, A. *Biomed. Res. Trace Elem.* **1992**, *3*, 257. (b) Agocs, L.; Burford, N.; Cameron, T. S.; Curtis, J. M.; Richardson, J. F.; Robertson, K. N.; Yhard, G. B. *J. Am. Chem. Soc.* **1996**, *118*, 3225. (c) Agocs, L.; Briand, G. G.; Burford, N.; Cameron, T. S.; Kwiatkowski, W.; Robertson, K. N. *Inorg. Chem.* **1997**, *36*, 2855. (d) Briand, G. G.; Burford, N.; Cameron, T. S.; Kwiatkowski, W. *J. Am. Chem. Soc.* **1998**, *120*, 11374.
(122) (a) Shibahara, T. In *Advances in Inorganic Chemistry*; Sykes, A., Ed; Academic Press: San Diego, 1991; Vol. 37, p 143. (b) Shibahara, T. *Coord. Chem. Rev.* **1993**, *123*, 73. (c) Sakane, G.; Shibahara, T. *ACS Symp. Ser.* **1996**, *653*, 225.
(123) Almén, T.; Berg, A.; Chang, C. A.; Droege, M.; Dugstad, H.; Fellmann, J. D.; Kim, S.-H.; Klaveness, J.; Rocklage, S.; Rongved, P.; Segal, B.; Watson, A. D. U.S. Patent 5,482,699, 1996.
(124) Novak, J.; Podlaha, J. *J. Inorg. Nucl. Chem.* **1974**, *36*, 1061.
(125) Soares, A. B.; Taylor, R. C.; Sykes, A. G. *J. Chem. Soc., Dalton Trans.* 1980, 1101.
(126) (a) Shibahara, T.; Kohda, K.; Ohtsuji, A.; Yasuda, K.; Kuroya, H. *J. Am. Chem. Soc.* **1986**, *108*, 2757. (b) Shibahara, T.; Yamasaki, M.; Sakane, G.; Minami, K.; Yabuki, T.; Ichimura, A. *Inorg. Chem.* **1992**, *31*, 640.
(127) Nasreldin, M.; Olatunji, A.; Dimmock, P. W.; Sykes, A. G. *J. Chem. Soc., Dalton Trans.* **1990**, 1765.
(128) Crystal data of $Na_2[W_2O_2S_2(EDTA)]\cdot 6H_2O$: Monoclinic, space group $P2_1/n$; $F_w = 906.1$ amu, $a = 14.007(3)$ Å, $b = 12.029(3)$ Å, $c = 27.399(6)$ Å, $b = 92.68(2)°$, $V = 4611(3)$ Å^3, $Z = 8$, $D_{calc} = 2.61$ g/cm^3, $\mu_{calc} = 104.7$ cm^{-1}, $T = -87$ °C. $R = 3.39\%$ and $R_w = 3.68\%$ with 5745 accepted unique reflections ($F^2 > 3\sigma(F^2)$) for 493 variables. Crystallographic data (excluding structure factors) for the structure reported in this paper have been deposited with the Cambridge Crystallographic Data Center as supplementary publication no. CCDC-125279. Copies of the data can be obtained free of charge on application to CCDC, 12 Union Road, Cambridge, CB2 1EZ, UK (fax: +44 1223−336−033; e-mail: deposit@ccdc.cam.ac.uk).
(129) Khalil, S.; Sheldrick, B. *Acta Crystallogr.* **1978**, *B34*, 3751.
(130) Ikari, S.; Sasaki, Y.; Ito, T. *Inorg. Chem.* **1989**, *28*, 447.
(131) Yamasaki, M.; Shibahara, T. *Inorg. Chim. Acta* **1993**, *205*, 45.
(132) Yu, S.-B.; Droege, M.; Segal, B.; Kim, S.-K.; Sanderson, T.; Fellmann, J.; Watson, A. *Book of Abstracts*, 212th ACS National Meeting, Orlando, FL, Aug. 1996, INOR-267.
(133) Yu, S.-B.; Droege, M.; Segal, B.; Downey, S.; Sanderson, T.; Fellmann, J.; Watson, A. *Inorg. Chim. Acta* **1997**, *263*, 61.
(134) Contant, R. In *Inorganic Synthesis*; Ginsberg, A. P., Ed; John-Wiley & Sons: New York, 1990; Vol. 27, p 104.
(135) Alizadeh, M. H.; Harmalker, S. P.; Jeannin, Y.; Martin-Frere, J.; Pope, M. T. *J. Am. Chem. Soc.* **1985**, *107*, 2662.
(136) Rhule, J. T.; Hill, C. L.; Judd, D. A.; Schinazi, R. F. *Chem. Rev.* **1998**, *98*, 327.
(137) (a) Katsoulis, D. E. *Chem. Rev.* **1998**, *98*, 359. (b) Pope, M. T. *Heteropoly and Isopoly Oxometalates*; Springer-Verlag: Berlin, 1983; p 31.
(138) Almén, T.; Berg, A.; Christoffersson, J.-O.; Droege, M.; Kim, S.-H.; Krautwurst, K.-D.; Segal. B.; Watson, A. D.; Yu, S.-B. Manuscript in preparation.
(139) Cotton, F. A. *Polyhedron* **1986**, *5*, 3.
(140) (a) Bino, A.; Cotton, F. A.; Dori, Z.; Koch, S.; Kuppers, H.; Millar, M.; Sekutowshi, J. C. *Inorg. Chem.* **1978**, *17*, 3245. (b) Ardon, M.; Cotton, F. A.; Dori, Z.; Fang, A.; Kapon, M.; Reisner, G. M.; Shaia, M. *J. Am. Chem. Soc.* **1982**, *104*, 5394. (c) Cotton, F. A.; Dori, Z.; Marler, D. O.; Schwotzer, W. *Inorg. Chem.* **1984**, *23*, 4738. (d) Bino, A.; Cotton, F. A.; Dori, Z.; Shaia-Gottlieb, M.; Kapon, M. *Inorg. Chem.* **1988**, *27*, 3592.
(141) Powell, G.; Richens, D. T. *Inorg. Chem.* **1993**, *32*, 4021.
(142) Cotton, F. A.; Wing, R. M.; Zimmerman, R. A. *Inorg. Chem.* **1967**, *6*, 11.
(143) (a) Hogue, R. D.; McCarley, R. E. *Inorg. Chem.* **1970**, *9*, 1354. (b) Dorman, W. C.; McCarley, R. E. *Inorg. Chem.* **1974**, *13*, 491.
(144) Hodali, H. A.; Hung, H.; Shriver, D. F. *Inorg. Chim. Acta* **1992**, *198−200*, 245.
(145) Mussell, R. D.; Nocera, D. G. *Inorg. Chem.* **1990**, *29*, 3711.
(146) Schoonover, J. R.; Zietlow, T. C.; Clark, D. L.; Heppert, J. A.; Chisholm, M. H.; Gray, H. B.; Sattelberger, A. P.; Woodruff, W. H. *Inorg. Chem.* **1996**, *35*, 6606.
(147) Kolesnichenko, V.; Messerle, L. *Inorg. Chem.* **1998**, *37*, 3660.
(148) Franolic, J. D.; Long, J. R.; Holm, R. H. *J. Am. Chem. Soc.* **1995**, *117*, 8139.
(149) Schulz, H. G.; Siepmann, R.; Schafer, H. J. *Less-common Met.* **1970**, *22*, 136.
(150) Downey, S.; Droege, M.; Yu S.-B.; Watson, A. D. Unpublished results.
(151) (a) Saito, T.; Yoshikawa, A.; Yamagata, T.; Imoto, H.; Unoura, K. *Inorg. Chem.* **1989**, *28*, 3558. (b) Saito, T.; Imoto, H. *Bull. Chem. Soc. Jpn.* **1996**, *69*, 2403.
(152) (a) Zhang, X.; McCarley, R. E. *Inorg. Chem.* **1995**, *34*, 2678. (b) Ehrlich, G. M.; Warren, C. J.; Vennos, D. A.; Ho, D. M.; Haushalter, R. C.; DiSalvo, F. J. *Inorg. Chem.* **1995**, *34*, 4454.
(153) (a) Kuhn, P. J.; McCarley, R. E. *Inorg. Chem.* **1965**, *4*, 1482. (b) Hughes, B. G.; Meyer, J. L.; Fleming, P. B.; McCarley, R. E. *Inorg. Chem.* **1970**, *9*, 1343.
(154) Kennedy, V. O.; Stern, C. L.; Shriver, D. F. *Inorg. Chem.* **1994**, *33*, 5967.
(155) (a) Uma, S.; Corbett, J. D. *Inorg. Chem.* **1998**, *37*, 1944. (b) Lulei, M.; Martin, J. D.; Hoistad, L. M.; Corbett, J. D. *J. Am. Chem. Soc.* **1997**, *119*, 513. (c) Ebihara, M.; Martin, J. D.; Corbett, J. D. *Inorg. Chem.* **1994**, *33*, 2079. (d) Park, Y.; Corbett, J. D. *Inorg.*

Chem. **1994**, *33*, 1705. (e) Llusar, R.; Corbett, J. D. *Inorg. Chem*. **1994**, *33*, 849. (f) Qi, R.-Y.; Corbett, J. D. Inorg. Chem. **1994**, *33*, 5727 (g) Corbett, J. D. *J. Alloys Compd*. **1995**, *229*, 10.

(156) Artelt, H. M.; Schleid, T.; Meyer, G. *Z. Anorg. Allg. Chem*. **1992**, *618*, 18. (b) Artelt, H. M.; Meyer, G. *Z. Anorg. Allg. Chem*. **1993**, *619*, 1.

(157) Long, J. R.; Zheng, Z.; Holm, R. H.; Yu, S.-B.; Droege, M.; Sanderson, W. A. U.S. Patent 5804161, 1998.

(158) Yaghi, O. M.; Scott, M. J.; Holm, R. H. *Inorg. Chem*. **1992**, *31*, 4778.

(159) (a) Long, J. R.; Williamson, A. S.; Holm, R. H. *Angew. Chem., Int. Ed. Engl*. **1995**, *34*, 226. (b) Long, J. R.; McCarty, L. S. Holm, R. H. *J. Am. Chem. Soc*. **1996**, *118*, 4603.

(160) Zheng, Z.; Long, J. R.; Holm, R. H. *J. Am. Chem. Soc*. **1997**, *119*, 2163.

(161) Willer, M. W.; Long, J. R.; McLauchlan, C. C.; Holm, R. H. *Inorg. Chem*. **1998**, *37*, 328.

(162) Zheng, Z.; Holm, R. H. *Inorg. Chem*. **1997**, *36*, 5173.

(163) Freedman, L. D.; Doak, G. O. *Chem. Rev*. **1982**, *82*, 15.

(164) Suzuki, H.; Maeda, K.; Tanikawa, K.; Miyaji, K. WO 95/06053.

(165) Chatterjee, G.; Cabasso, I.; Smid, J. *J. Appl. Polym. Sci*. **1995**, *55*, 851.

(166) (a) Delaviz, Y.; Zhang, Z.-X.; Cabasso, I.; Smid, J. *J. Appl. Polym. Sci*. **1990**, *40*, 851. (b) Ignatious, F.; Sein, A.; Delaviz, Y.; Cabasso, I.; Smid, J. *Polymer* **1992**, *33*, 851. (c) Chatterjee, G.; Ignatious, F.; Cabasso, I.; Smid, J. *Polymer* **1995**, *36*, 851.

(167) Rawls, H. R.; Marshall, M. V.; Cardenas, H. L.; Bhagat, H. R.; Cabasso, I. *Dent. Mater*. **1992**, *8*, 54.

(168) Klaveness, J.; Berg, A.; Almén, T.; Golman, K.; Droege, M.; Yu, S.-B. U.S. Patent 5,817,289, 1998; *Chem. Abstr*. **1959**, *125*.

CR980441P